A Review of Medical Image Registration

Calvin R. Maurer, Jr., MS
Department of Biomedical Engineering

J. Michael Fitzpatrick, PhD
Department of Computer Science

Vanderbilt University
Nashville, Tennessee 37235

January 28, 1993

[A version of this manuscript appeared as a chapter in the book: R. J. Maciunas, editor. *Interactive Image-Guided Neurosurgery.* Park Ridge, IL: American Association of Neurological Surgeons, 1993, pp. 17–44.]

Introduction

The ever expanding gamut of medical imaging techniques provides the clinician an increasingly multifaceted view of brain function and anatomy. The information provided by the various imaging modalities is often complementary (i.e. provides separate but useful information) and synergistic (i.e. the combination of information provides useful extra information). For example, X-ray computed tomography (CT) and magnetic resonance (MR) imaging exquisitely demonstrate brain anatomy but provide little functional information. Positron emission tomography (PET) and single photon emission computed tomography (SPECT) scans display aspects of brain function and allow metabolic measurements but poorly delineate anatomy. Furthermore, CT and MR images describe complementary morphologic features. For example, bone and calcifications are best seen on CT images, while soft-tissue structures are better differentiated by MR imaging. Clinical diagnosis and therapy planning and evaluation are increasingly based on this complementary image information.

In the past it has been common for physicians to interpret data from different modalities, recorded at different times, using a poorly described yet generally understood visual alignment system. This in effect involves applying some spatial transformation between structures within an image in order to match the data. In the last several several years, there has been a large amount of effort spent developing more objective methods of aligning image information. In order to relate the information in one image to information in another image, it is necessary to establish a one-to-one mapping between the points in each image. The mapping can be partial or complete, but it must include all points of diagnostic or surgical interest to be useful. As defined in the next section, we use the term *registration* to mean the determination of a transformation from one space to another. When the transformation has been determined we say that the images are *registered*.

Registration techniques make it possible to superimpose features from one imaging study over those of another study. For example, skeletal structures and areas of contrast enhancement seen in CT images can be overlaid on MR images which clearly depict soft-tissue anatomy. Likewise, functional lesions detected with PET can be viewed in the context of brain anatomy imaged with MR. This process can also be applied to multiple data sets obtained with the same modality at different times in order to bring the images into registration for the purpose of quantitative comparison, which increases the precision of treatment monitoring with serial images.

Registration techniques have recently been extended to relate image space to physical space. Stereotactic surgery and stereotactic radiosurgery require that an image or images be registered with the physical space occupied by the patient during surgery. An emerging interactive, image-guided surgery technology uses image-to-physical space registration to reflect the current surgical position on a display of the preoperative image set(s) of that patient.

This review is organized as follows. First, we define registration and examine its relationship to reformatting and rendering. After we discuss methods of classifying registration techniques and make a few general comments about transformations, we present a comprehensive literature review of techniques that have been used to register images to other images, to physical space, and to anatomical atlases. We then note that image registration strongly depends on the quality of the images and discuss the avoidance and correction of

image distortion. Finally, we compare registration methods, noting some of their uses and relative advantages. We restrict the discussion to methods that register images after they are acquired, i.e. we do not consider patient alignment prior to imaging [34, 106, 115, 141, 142]. We emphasize those techniques that appear to be most useful to neurosurgeons.

Registration versus Reformatting and Rendering

Image registration should be distinguished from two related concepts—image reformatting and image rendering. These three "Rs"—registration, reformatting, and rendering—are often used within the same context in the medical imaging literature and can lead to confusion, particularly with respect to the first two. We will therefore define these terms and examine their relationships with some care before we begin our survey. Before we define these concepts we define what we mean by an image. We are concerned primarily with medical images, by which we mean either tomographic images, such as CT, MR, PET, SPECT, and B-mode ultrasound, or projection images, such as conventional X-ray and scintigraphic images. We are less concerned with photographic images, which are shaded and possibly colored images of surfaces. In this context we define an *image* as a two-dimensional or three-dimensional pattern of intensity. The intensity will be a number, such as the CT number or the number of scintigraphic counts, and there will be a number associated with each point in the image space. The pattern is typically displayed by assigning different levels of brightness, known as *gray levels*, to represent different intensities, but in some cases, for example PET images, the gray levels may be replaced by colors. Since these colors are not related to the physical color of the object being imaged they are known as *pseudocolors*. Because we are interested in geometrical measurements, we will impose a coordinate system on each image space. The points in the space are specified in the usual way for two-dimensional images by means of two Cartesian coordinates, which are the distances, x and y, from two perpendicular axes, and for three-dimensional images, also known as *volume images*, by the distances, x, y, and z, from three perpendicular planes. Examples of the coordinates can be seen in Figures 1A and 1B.

Registration. We define registration as the *determination of a one-to-one mapping between the coordinates in one space and those in another such that points in the two spaces that correspond to the same anatomical point are mapped to each other.* The mappings, which are also called *transformations*, are two dimensional for two-dimensional spaces and three dimensional for three-dimensional spaces. The simplest examples are the rigid body transformations, which are transformations in which the distances among all points are preserved. The rigid transformations are typically used to compensate for different imaging orientations of rigid objects. More complicated mappings may be used to compensate for elastic motion of the objects between the acquisition of two images. Elastic mappings may also be used to correct for erroneous warping caused by imperfections in the imaging process, but such corrections properly fall under the general class of image *restoration*, which includes processing to correct for any degradation, and under the more specific class of image *rectification*, which is restoration that corrects for geometric distortion.

An example of a two-dimensional registration employing a rigid body transformation is shown in Figure 1. Figures 1A and 1B show schematically two images of the same two-dimensional object acquired with the same or different modalities. The images differ in two obvious ways. First, the orientation of the object is different and, second, part of the object has been removed in the image in Figure 1B. Image 1A has been rotated so that the object appears on the page in the same orientation as in 1B to emphasize the difference in orientation of the image spaces relative to the object as opposed to the difference in orientation of the object relative to the image spaces. The images may have been acquired

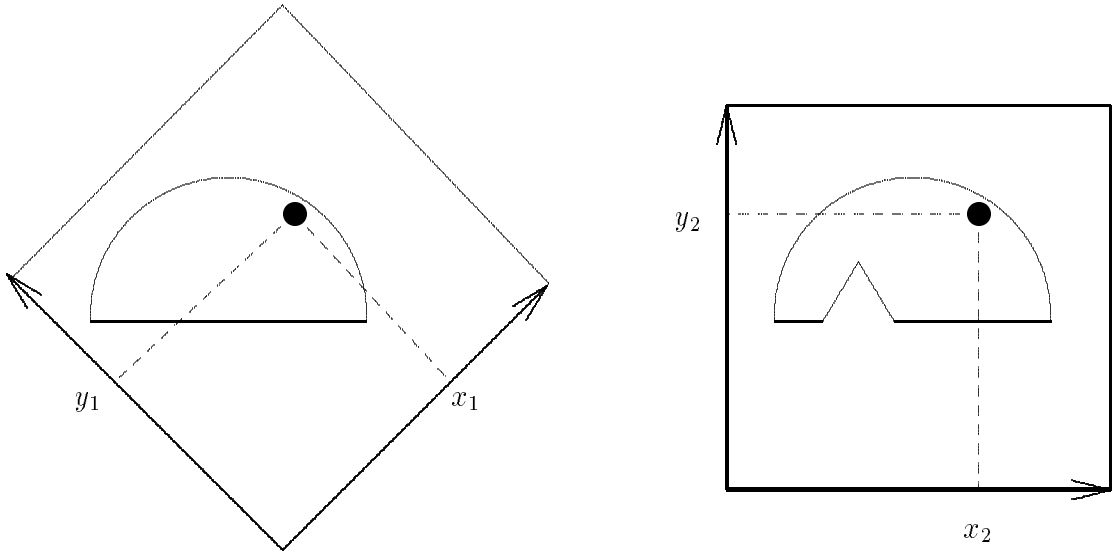

1A 1B

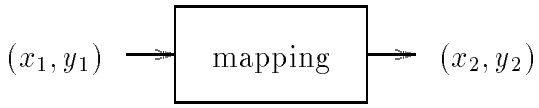

1C

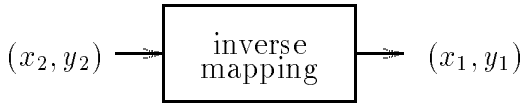

1D

Figure 1: *Registration.* 1A: An image of some object. 1B: A second image of the same object acquired at a different orientation. Image 1A has been rotated so that the object appears in the same orientation as in 1B. Image 1B reveals that part of the object has been removed between image acquisitions. The black dot in each image corresponds to the same anatomical point in the object. The origin of the x, y coordinate system is at the bottom corner in 1A and at the lower left corner in 1B. 1C: Schematic illustration of the process of mapping in two-dimensional space. Each point (x_1, y_1) in the space of image 1A is mapped into a unique point (x_2, y_2) in the space of image 1B. 1D: The equivalent inverse mapping in which points in space two are mapped into points in space one.

with the same or different imaging modalities. They may, for example, represent two CT images acquired of a patient's head before and after surgery, in which case the missing piece might represent a resection. They may on the other hand represent two images acquired with different modalities, MR and PET, for example, in which case the missing piece illustrates the difference in image patterns produced by the two modalities. Figures 1C and 1D show schematically the process of mapping points between the two image spaces. Each point (x_1, y_1) in the space of image one is mapped into a unique point (x_2, y_2) in the space of image two. The forward mapping is shown in 1C and the inverse mapping in 1D. If the mapping is physically reasonable the mapping will be one-to-one, meaning that each point in one space is paired with exactly one point in the other space. The black dots represent points in the two image spaces that correspond to the same anatomical point. If all such points, or at least all points of diagnostic or surgical interest, are mapped together, or at least approximately together, then the mapping qualifies as a registration. The images in Figures 1A and 1B represent two orientations of the same rigid object. Thus, the mapping that effects the registration will be a rigid body transformation. While there is nothing in Figure 1 that indicates whether or not the mapping is a registration, we will assume henceforth that it is. It is important to note here that in some circumstances part of the object may take part in non-rigid motion while the rest of the object moves rigidly. An important example is the head. The skull and much of the brain will typically move as a rigid, or approximately rigid, object, while some parts of the brain, particularly areas near a resection, may move elastically. In such cases the term registration would typically apply to a rigid mapping that registers the rigid component of the object, but it may be more appropriate in some situations to use an elastic mapping that registers both components.

While our discussion of registration has focused on image-to-image registration, it is crucial that we enlarge the definition of registration to include image-to-object registration as well. To illustrate image-to-object registration we let the image of Figure 1B represent the actual object, as opposed to an image of the object. The coordinates x_2 and y_2 now represent the coordinates of the physical space in which the object is immersed. These coordinates must be measured by means of some physical device present in the vicinity of the object. Typically the device can approach only the surface of the object and can therefore measure the position of far fewer points than a tomographic imager, but nonetheless the rest of the registration scheme is the same. Stereotactic neurosurgery, in which an image of anatomy is registered with the anatomy itself for the purpose of targeting deep-seated lesions is the most common application, but in one way or another all of image-guided neurosurgery relies on the registration of the image of an object to the object itself.

Reformatting. We define the reformatting of an image as *the mapping of image intensities onto points in a space that has been rotated and possibly shifted relative to the space in which the image was originally acquired.* Common examples are the determination of the coronal or sagittal views of a volume image that was obtained in the axial orientation. In that case the orientation of the new space differs from that of the original space by a 90 degree rotation. It is illuminating to note that reformatting produces a new image, whereas registration does not. However, it is often convenient to reformat an image after it has been registered to some target image via a rigid transformation. Figure 2 illustrates this process. The image in Figure 2A is a copy of that in Figure 1A and is an image acquired by means of some unspecified imaging modality. The image in Figure 2B is a reformatted version of 2A.

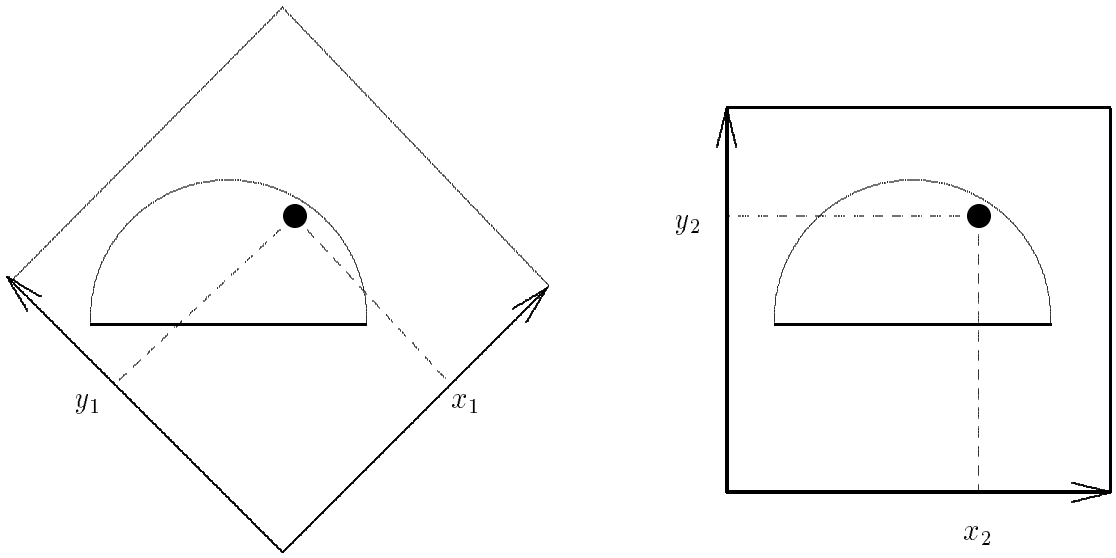

Figure 2: *Reformatting.* 2A: A copy of the image in Figure 1A. 2B: A reformatted version of 2A. The black dot in each image corresponds to the same point in the two image patterns. As in Figures 1A and 1B the origin of the x, y coordinate system is at the bottom corner in 2A and at the lower left corner in 2B.

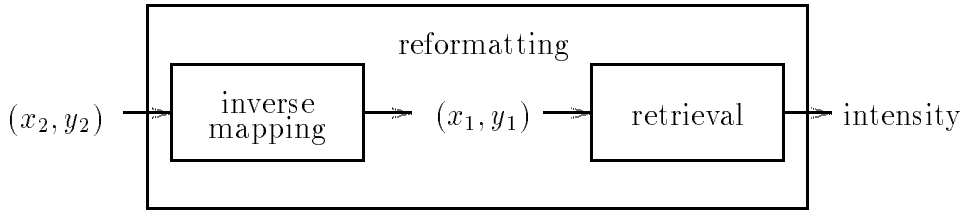

2C

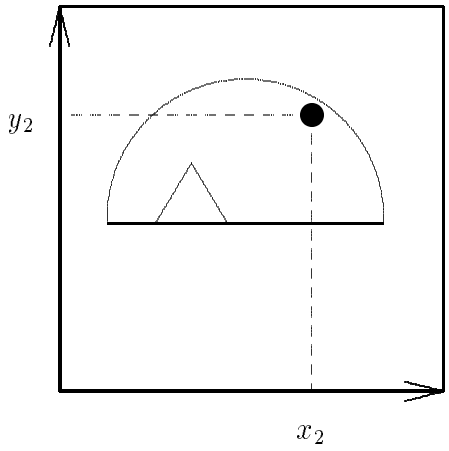

2D

Figure 2: *Reformatting* (continued). 2C: Schematic illustration of the process of reformatting in continuous two-dimensional space. Reformatting involves point mapping followed by a retrieval of image intensity from the mapped point. 2D: A superposition of image 2B with the image in Figure 1B. It can be seen that the reformatting made use of the point mapping that registers the two images in Figures 1A and 1B.

Figure 2C shows schematically the process of reformatting. An arbitrary point in the new space is represented by (x_2, y_2), and it corresponds to some point (x_1, y_1) in the space of 2A. Because only rotation and shifting are involved, the mapping from 2A to 2B and the inverse mapping from 2B to 2A are rigid transformations. To effect the reformatting two steps are required for every point (x, y) in the new image. First the corresponding point (x_1, y_1) in the acquired image must be determined by applying the inverse mapping and then the intensity in the acquired image at that point must be retrieved. When this process has been carried out for every point the reformatting is complete. The orientation of the reformatted image is determined entirely by the mapping used in the first step. If for example the new space is rotated by 180 degrees about the center of the image relative to the space of the acquired image, the reformatted image will be upside down. It is implicit in our definition of reformatting that the mapping must be a rigid transformation and that mirroring is excluded, since mirror images cannot be produced by rotations and translations. It may be appropriate in some contexts to generalize the notion of reformatting to include arbitrary mappings in the first step, but we choose to use the more common, limited definition.

So far our discussion of Figure 2 does not distinguish between reformattings that correspond to registrations and other reformattings. The distinction lies in the mapping chosen in the first step in 2C. If the mapping is one that produces a registration between 2A and some target image, then the reformatting will correspond to that registration. Let us suppose that the mapping used in Figure 2 is the same one used in Figure 1 to register 1A with 1B. Then if we superimpose the reformatted image 2B with the target image 1B we will see an image like the one in 2D. As discussed above, the two images, 1A and 1B may have been acquired with the same or different imaging modalities. For the case of the pre- and postoperative CT images the superimposition makes it easy to see which tissue has been resected. For the case of the MR and PET images, the anatomy depicted by the MR image provides context for the functional PET image.

Now that we have distinguished between reformatting for registration and other reformattings, it is possible to combine these two ideas. It might for example be convenient to see superimposed sagittal views of a pair of axial CT and MR volume images. The registration step would provide a mapping between the axial views. That mapping could then be composed with a mapping that produces an axial-to-sagittal rotation. If the resulting composition is used to reformat the MR image, say, and the axial-to-sagittal mapping alone is used to reformat the CT image, the result would be two reformatted images that were not only registered but also conveniently oriented. This idea is also appropriate for image-to-object registrations. Here it might be desirable to register an axial CT volume image of the head to the head itself for surgical guidance. Furthermore, it might be convenient to have the images presented during surgery at an orientation that agrees with the view of the surgeon during the planned approach to the lesion. To provide the appropriate images it would be necessary to determine the mapping that registers the CT volume image to the head and then determine the mapping that rotates the axial view to the view of the approach. The composition of these two mappings would be used in the first step of the reformatting to produce a conveniently oriented, registered volume image.

We have in our discussion of reformatting avoided a complication associated with reformatting that arises from the digital nature of the acquired images. All medical imaging modalities that yield volume images produce digital images. There are two aspects to the

digital nature of these images. The first aspect is *spatial quantization*, also known as *sampling*. Because of sampling, the image, rather than being a continuous pattern of intensity, is composed of a discrete array of sampled intensities, called *voxels* for "volume element" for three-dimensional images or *pixels* for "picture element" for two-dimensional images. In this sense the image is more like a mosaic than a photograph. (In this work we typically use the term voxel when the number of dimensions is unspecified.) The second aspect, called *quantization*, is the discrete nature of the intensity stored at each pixel or voxel. The intensity is encoded as an integer, which means that it is not possible to store fractional values. The complication caused by the digital nature results from the sampling. It occurs at the second step of the reformatting process in which the image intensity is retrieved from the acquired image. The problem, illustrated in Figure 3, is that the point (x_1, y_1) at which an intensity value is to be retrieved may not be one of the sampled points in the image. This situation develops for at least some of the voxels when the mapping is a rotation by other than a multiple of 90 degrees or when the mapping includes a shift of a fraction of the dimension of voxel. In Figure 3, for example, there is a rotation of about 45 degrees between images 3A and 3B, and it can be seen that the mapping from (x_2, y_2) in image 3B goes to a position (x_1, y_1) in image 3A that is not one of the sampled positions. Thus, there is no image intensity to retrieve at the mapped position in image 3A. It is necessary to estimate the intensity at (x_1, y_1) by interpolating from the other pixels in the neighborhood. The four $\times$s shown in 3A are examples of a set of pixels that might be used for interpolation. This process of determining intensities at new positions in a digital image is called *resampling*. Resampling is also employed when it is desired to change the size of voxels in a digital image. For example if a 256 by 256 voxel MR image whose voxels are 1.5 mm by 1.5 mm by 4 mm in size has been acquired and it is desired to produce a 512 by 512 voxel MR image with 0.75 mm by 0.75 mm by 4 mm voxels it would be necessary to resample. Resampling is also necessary when it is desired to overlay two registered images when the voxel dimensions are different. The subject of resampling has been studied in the field of computer graphics and well understood. An excellent survey of the field has been provided by Wolberg [196].

Rendering. The third "R" is rendering. We define rendering as *the simulation of a photograph of a three-dimensional opaque or translucent surface or surfaces defined within a volume image.* A typical example is the rendering of the outer surface of the skull in a CT volume image of the head. The surface that is rendered may be associated with a physical surface, as with the skull, but it does not have to be. It is typically defined in terms of the patterns of intensity in the image. With the skull in a CT volume for example, bone might be identified as occupying all points whose intensity is above some specified threshold. The definition of the outer surface of the skull would then be the set of all such voxels visible from some specified vantage point in the image space lying outside the head. The visibility is determined geometrically. A popular technique to determine visibility, illustrated schematically in Figure 4, is *ray tracing*, in which rays from the chosen vantage point are traced through the region occupied by the object. In the figure the hemispherical surface represents the surface whose points match the definition of the outer skull surface for some particular CT volume image. The first voxel containing bone on each ray would be part of the outer skull surface. For the ray shown in Figure 4, the first voxel is at position 1. The second voxel, at position 2, would be hidden by the first voxel and therefore would not be visible in the simulated photograph. (Note that it would not be necessary to continue the

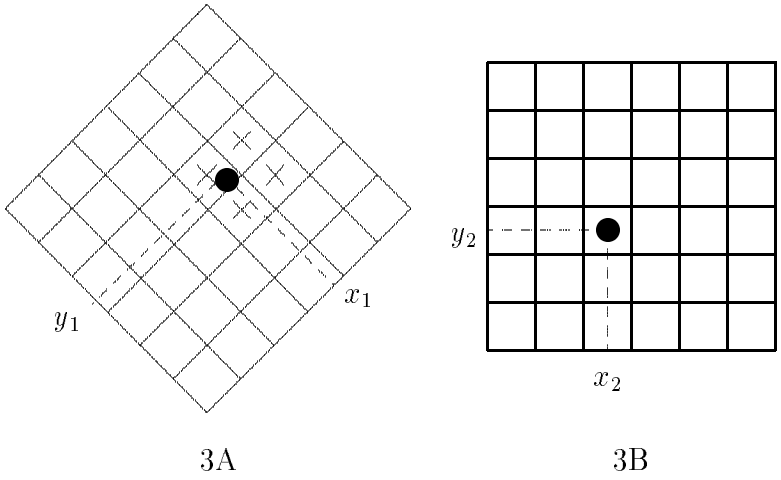

Figure 3: *Digital Sampling.* 3A and 3B are enlarged views of small portions of the two-dimensional images in Figure 2A and 2B, respectively. The images are assumed to be digital and the squares are pixels that make up the image. A mapping from (x_2, y_2) to (x_1, y_1) is shown for which (x_1, y_1) is not a sampled point in 3A. The $\times$s are sampled points that have been chosen for the interpolation.

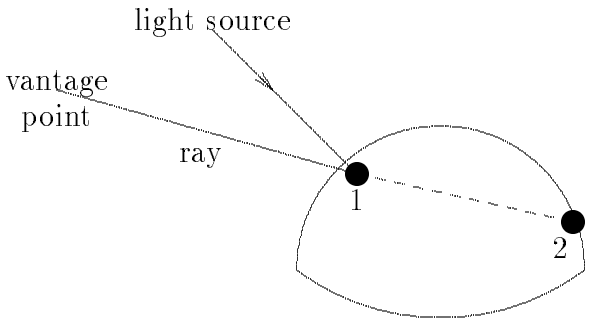

Figure 4: *Rendering.* A schematic depiction of the process or ray tracing for the purpose of image rendering. The hemispherical surface is being rendered by tracing rays from the vantage point. The shading is determined according to the position of the simulated light source. One ray is shown passing through points 1 and 2. Since point 2 is hidden by point 1, it will not be visible in the rendering.

tracing along the dotted portion of the line.) The rays are directed oppositely to the direction along which simulated light would travel from the imaged object back to an observer whose eye is located at the vantage point. The simulation of the photograph would be based on the shape of this surface and the chosen position of a light source or sources. The angle relative to the surface at which the light strikes the surface and the angle at which the reflected light leaves the surface are used in the simulation to determine the apparent brightness of each point on the visible surface. The result is a pattern of shading from which the observer can intuitively appreciate the shape of the surface. A surface may also be defined as the locus of points for which the intensity is below some threshold or within some bounds or at which the image intensity pattern exhibits a large change or a strong texture, etc. Finally, if no such algorithmic definition is available, as is often the case for anatomical surfaces, the surface may be defined as the voxels identified in the image volume by an observer. Alternatively the surface may be unrelated to any image at all, but defined in terms of some calculated values, such as the radiation dose for radiotherapy or radiosurgery.

Rendering is one step removed from the original or reformatted intensity pattern because of the need for a definition of the surface or surfaces. Furthermore, it reveals only qualitative information about shape of the surfaces and nothing about the anatomy behind them. Its purpose is simply to provide cues to assist the observer in recognizing the orientation of defined surfaces and to appreciate their three-dimensional shapes. It may be helpful, for instance, to provide the neurosurgeon with a rendered skull image in order to make the orientation of the head easier to visualize. It may even be helpful to present a rendering of the surface of a lesion, but it serves only as an adjunct to the intensity pattern itself. Rendering is related to registration in two ways. First, the registration of two images makes it possible to combine two or more renderings into one simulated photograph. For example, it may be desirable to show a rendered skull with a section removed to reveal the surface of the brain. The skull rendering would be derived from a CT volume, while the brain rendering might be derived from an MR volume. Before these renderings were performed it would be necessary to register the CT volume with the MR volume. (No reformatting need be done.) The mapping that registers the two volumes would then be used to map the vantage point and the viewing direction in one volume to the corresponding vantage point and viewing direction in the other volume. Once these correspondences are established the resulting renderings can be carried out individually and will be registered so that they can be combined. Such renderings of collections of surfaces can be extended to include the surfaces of lesions and other critical structures, but it should be emphasized that rendering does not assist in the detection of such structures, but only in the depiction of their surfaces after they have been detected. Second, rendering can provide assistance in the registration process. In some interactive techniques, rendered views provide visual cues that enable the user to identify and align corresponding anatomical points or surfaces.

The usefulness of rendering is increased if it is made *interactive*, which means that the user is able to strike a key, turn a dial, slide a mouse, or move a joystick, etc., to select a new orientation. Interactive rendering would be necessary, for example, in the registration techniques that require user assistance. It may also be convenient to use rendering in an interactive mode to allow a surgeon to choose an orientation preoperatively. The surgeon would view a rendered image of the skull, brain, or other anatomical surface or combination of surfaces at some orientation and move a mouse or joystick to see other orientations. The

usefulness of interactive rendering is increased dramatically if it can be done in *real time*, which means that renderings from new vantage points are computed so quickly that the motion appears to be as smooth as it would if it were seen in a movie of a moving object. Because the computations necessary for rendering are complex, real time rendering requires computers with high speed hardware specialized for the computational tasks peculiar to rendering.

The study and development of rendering techniques are part of the active and growing field of *volume visualization.* The reader is directed to the proceedings of the recent SPIE conference on this subject [161] and to the recent work by Udupa [184] for further study.

Classification of Registration Methods and General Comments

Gerlot-Chiron and Bizais have presented a unified description of existing registration methods [68, 69, 70]. They propose the following general registration technique methodology: (1) extraction of features in each image, (2) pairing of these features, (3) choice of a geometric transformation and estimation of its parameters, and (4) effectuation of this transformation. They classify registration methods into four categories, in which the above four steps are implemented differently: (1) point methods, (2) edge methods, (3) moment methods, and (4) "similarity criterion optimization" methods. Van den Elsen et al. have also recently presented an extensive classification scheme for registration methods [187]. They classify techniques according to a number of criteria: (1) dimensionality (1D vs. 2D vs. 3D vs. 4D), (2) type of features using for registration (intrinsic vs. extrinsic), (3) domain of the transformation (local vs. global), (4) type of transformation (rigid vs. affine vs. projective vs. curved), (5) parameter determination (search vs. closed-form solution), and (6) interaction (interactive vs. semi-automatic vs. automatic).

We divide our review of registration techniques into several sections in a manner roughly similar to that of Gerlot-Chiron and Bizais: (1) stereotactic frame systems, (2) point methods, (3) curve and surface methods, (4) moment and principal axes methods, (5) correlation methods, (6) interactive methods, and (7) atlas methods.

Given two images $I_1(x_1, y_1, z_1)$ and $I_2(x_2, y_2, z_2)$ which were obtained by imaging the same object at different times and/or in different modalities, we wish to find a mapping $\mathcal{F} : (x_1, y_1, z_1) \mapsto (x_2, y_2, z_2)$ that maps every point of one image onto a unique point in the second image. Registration involves identifying this mapping $\mathcal{F}$. The mapping $\mathcal{F}$ is generally chosen from a parametric family of transforms. Thus the central problem in registration, after extracting and pairing common features, is the choice of this parametric transformation and the estimation of its parameters. The advantage of the parametric approach is that it avoids several well known problems of interpolation, including occasional "overshoots" due to smoothing and the arbitrary determination of various "stiffness" parameters.

Rigid body motion is often assumed when registering volume images of the head. This assumption arises from the presumption that the head is approximately a rigid body, which is defined in classical mechanics as a "system of particles whose mutual distances are all constant" [177]; that the patient's head was imaged in different orientations; and that the different imaging devices have identical magnification. Rigid body motion can be decomposed into a rotation and a translation. There are many ways to represent rotation, including Euler angles, axis-and-angle systems, orthonormal matrices, unit quaternions, Cayley-Klein parameters, Gibbs vectors, and Pauli spin matrices [5]. Orthonormal matrices are used most often in graphics, robotics, and photogrammetry. Using matrices, any rigid body transformation can be represented by

$$\mathcal{F}(\mathbf{x}) = \mathbf{A}\mathbf{x} + \mathbf{b} \tag{1}$$

where $\mathbf{x} = (x, y, z)$, $\mathbf{A}$ is the 3x3 rotation matrix, and $\mathbf{b}$ is the 3x1 translation vector. The matrix $\mathbf{A}$ is constrained by

$$\mathbf{A}^T\mathbf{A} = \mathbf{I}, \quad \det \mathbf{A} = 1 \tag{2}$$

where $\mathbf{I}$ is the 3x3 identity matrix. The constraint $\det \mathbf{A} = 1$ insures that the rotation is a proper rotation. The possibility $\det \mathbf{A} = -1$ represents an improper rotation (reflection, inversion).

Without the constraints (2), equation (1) represents an affine transformation. Affine transformations map straight lines to straight lines and preserve parallelism. Examples of affine transformations are uniform (isotropic) scaling, non-uniform (anisotropic) scaling, and shearing. If the constraints (2) are replaced by

$$\mathbf{A}^T\mathbf{A} = \sigma^2\mathbf{I}, \quad \det \mathbf{A} = \sigma^n \tag{3}$$

where σ is a positive geometrical scaling constant and n is the image dimension, then equation (1) represents uniform scaling. Uniform geometrical scaling is sometimes necessary for photographic images based on the use of a lens system because there is a direct relationship between the size of the object in the image and the distance between the object and the optical device. General affine transformations can correct for certain image device distortions, e.g. shearing due to a tilted gantry in CT or distortion due to gradient coil imperfections in MR.

Another useful transformation is the projective transformation, which can be represented by a linear matrix transformation in the next higher dimension. Projective transformations, like affine transformations, map straight lines to straight lines, but unlike affine transformations, do not preserve parallelism. These transformations are useful for registering two-dimensional projection images to three-dimensional volume images.

Nonlinear transformations, which map straight lines to curves, are also sometimes useful. The best known nonlinear transformations used in image registration are polynomial functions. Linear [53, 73, 137, 174], quadratic [197], cubic [74], and higher order polynomials [191] have been used to match images. Other nonlinear transformations that have been explored are exponential warping [199] and "thin-plate splines" [18]. Nonlinear transformations are useful for deforming an anatomical atlas to fit image data. They are also useful for registering images of globally deformable anatomy such as the abdomen and chest. Finally, nonlinear transformations, in conjunction with rigid body transformations, are potentially useful for registering images that represent primarily rigid body motion with some local deformation. For example, the skull and much of the brain generally move as an approximately rigid object while some parts of the brain, e.g. near a resection, may move elastically.

Stereotactic Frame Systems

A stereotactic frame is a mechanical device used for the accurate positioning of instruments such as probes, electrodes, and biopsy cannulas in three-dimensional space. Although the use of mechanical guidance devices for the placement of intracranial probes was first reported in the latter half of the 19th century by Dittmar [41] and Zernov [100], Horsley and Clarke are generally credited with the development of stereotaxy. They described a stereotactic apparatus and atlas, based on cranial landmarks, developed for the systematic functional exploration of cerebellar function in small animals [29, 92]. Their device attached to the animal's skull by means of bars inserted into the external auditory canals and fixed to the intraorbital ridge and hard palate. The cranial fixation points established a three-dimensional stereotactic coordinate system formed by the canthomeatal line, the infraorbital line, and the midline.

An adaptation of their device was developed by Mussen for use in humans but was probably never used [148]. In humans, the relationship between the location of subcortical structures and cranial structures is more complicated than in animals. Too much spatial variability exists between individual human brains to safely rely on cranial landmarks to locate subcortical targets. The first human stereotactic operation was performed by Spiegel and Wycis in 1947 [173]. They developed a stereotactic atlas based on ventricular system landmarks [172]. Anatomical targets were located relative to the pineal gland and foramen of Monro visualized by preoperative or intraoperative pneumoencephalograms.

Current stereotactic systems embody several features: a stereotactic reference frame which provides rigid skull fixation using pins or screws and establishes a stereotactic coordinate system in physical space, a method for stereotactic image acquisition, and a system for mechanical direction of a probe or other surgical instrument to a defined intracranial target point. The Brown-Roberts-Wells (BRW) system was the first frame specifically designed to use CT volume images [20, 21, 22]. This system essentially consists of a head ring, an image localizing system, and a mechanical arc-guidance system. The head ring is attached to the skull with penetrating pins. The image localizing system consists of six vertical and three diagonal carbon fiber rods which form three N-shaped figures. This image localizing device is attached to the head ring during CT image acquisition. The rods appear as nine fiducial marks arranged around the periphery of each image slice. The positions of these fiducial points determine the position and orientation of each slice and are used to calculate the positions of targets in the physical space coordinate system defined by the head ring. These calculated target positions can be used to accurately position surgical probes and instruments using the polar coordinate guidance frame. Other popular stereotactic systems, e.g. the Leksell system [122] and the Todd-Wells system [72], have been modified to incorporate CT volume images using the N-shaped fiducial approach. More recently, these systems have been modified to incorporate MR [83, 109, 110, 121, 123, 130, 155] and PET [109, 110, 132, 201] images. MR images are acquired after filling hollow N-shaped tubes with petroleum jelly or an aqueous solution of copper sulfate or gadolinium. PET images are obtained using fluorine 18 [132] or germanium 68 [201] to fill the tubes. These modified stereotactic systems allow the registration of multimodality image volumes acquired with the frame attached.

Frame systems have several advantages: they are very accurate and they are immune

to several types of image distortion, including geometric scaling and shearing due to gantry tilt. The primary disadvantages of frame systems are that they are somewhat difficult to learn to use, they cannot incorporate scans acquired before the frame was applied, they are somewhat cumbersome, and their use is limited to surgery since the fixation technique is invasive.

Stereotactic frames are used for a wide variety of applications, including lesion biopsy, ventriculostomy, and radiosurgery [108]. Neurosurgical planning software tools have been developed that allow neurosurgeons to correlate corresponding points in various images and to reconstruct oblique image slices to examine different biopsy trajectories [138, 158]. Stereotactic radiosurgery treatment planning systems have been reported that display isodose contours on images from various modalities [165]. Frames have also been used to investigate the possibilities of interactive, image-guided surgery [99, 138]. The image-to-physical space registration provided by the stereotactic frame is used to update the current position of a surgical probe on a display of preoperative image sets of that patient.

The ability of stereotactic frames to localize intracranial image targets in the stereotactic coordinate space is limited by the image resolution. The accuracy of stereotactic systems is approximately one half of the slice thickness of the image slices, except for very thin slices [61, 131].

The reader interested in further details is referred to a number of excellent reviews and surveys [59, 82, 101, 107, 108].

Point Methods

Point methods involve the determination of the coordinates of corresponding points in different images and/or physical space and the estimation of the geometric transformation using these corresponding points. The points may be either intrinsic [16, 45, 49, 55, 79, 86, 87, 88, 111, 119, 124, 133, 134, 139, 171], extrinsic [3, 14, 30, 47, 49, 56, 58, 60, 79, 80, 81, 105, 114, 116, 135, 136, 149, 151, 163, 164, 178, 188, 189, 190, 198] or a combination of both [117, 118]. Intrinsic points are derived from patient specific image properties, e.g. anatomical landmark points. Extrinsic points are derived from artificially applied markers, e.g. glass beads.

Selection of appropriate points is a key factor in the success of a registration using intrinsic points. Anatomic landmark selection is a labor intensive, interactive process [45, 49, 86, 87, 88]. Points must be easily defined in three dimensions and must correspond to a well-defined landmark visible in both imaging modalities. Hill et al. suggest several possibilities: a point anatomical structure, e.g. the apical turn of the cochlea; the intersection of two linear structures, e.g. a blood vessel bifurcation or confluence; a particular topographic feature on a surface, e.g. an identifiable part of a sulcus or gyrus; the intersection of a surface structure with a linear structure, e.g. where a nerve passes through a foramen; and the intersection of three surface structures [86, 87, 88].

A wide variety of extrinsic markers have been used to register CT, MR, PET, and/or SPECT images with each other and/or with physical space. Investigators have used tubes containing copper sulfate ($CuSO_4$) [30, 164], glass beads [56], vitamin E tablets [56], tubes filled with oil [58], staples [60], spheres containing $CuSO_4$ and technetium 99m (^{99m}Tc) [79, 80], chrome alloy spheres [81], gelatin spheres [135, 136], polyvinyl alcohol gel markers [178], large V-shaped markers containing an aqueous solution of gadolinium [114, 188, 189, 190], and circular disks containing ^{99m}Tc [114, 188, 189, 190].

A good extrinsic marker needs to be accurately detectable in all image modalities being considered. For example, oil should not be used as a marker in MR images to avoid the phenomena of chemical shift which causes translational displacement in the image [30]. It is important to carefully define what point derived from the extrinsic marker is going to be used for registration. Mandava et al. call the points used for registration *fiducial points* or *fiducials*, as distinguished from "fiducial markers", and pick as their fiducials the geometric centers of the markers [135, 136]. Van den Elsen et al. use large V-shaped markers and pick as their fiducials the intersection of the axes of the tubes comprising the sides of the markers [114, 188, 189, 190].

Estimating the coordinates of the fiducials, which we call *fiducial localization*, can be manual or semi-automatic. Mandava et al. [135, 136] and DeSoto et al. [39] have presented semi-automatic fiducial localization techniques that use adaptive intensity-based segmentation algorithms. The markers are segmented from background in a user-defined region of interest by an algorithmically generated intensity threshold [104, 113]. The fiducial position of a marker is then estimated as the intensity-weighted average of all the voxel locations determined by the segmentation algorithm to contain marker.

The physical space coordinates of extrinsic markers have been determined by touching the markers with an articulated arm [3, 60, 116, 178] or a "low-frequency magnetic field 3-D digitizer" [105], observing the markers in a stereoscopic microscope [163], and ultrasonic rangefinding [56]. Lewis and Galloway recently presented a technique based on the reflected

A-mode ultrasound signal for transcutaneously localizing small plastic cylinders implanted in pork scapula [128]. Haynor et al. determined the coordinates of 2 mm chrome alloy markers using stereo photogrammetry techniques [81]. Briefly, if an object is identified on two projection films taken at different angles, its location must be at the intersection of the two lines connecting the two positions of the focal spot with the respective locations in the room of the image of the object.

Extrinsic point registration methods have several advantages. Any image modality can be registered as long as a marker can be constructed that is detectable in its images. Extracting extrinsic marker positions from medical images is often easier than extracting patient related image properties because the design of the markers can be optimized for automatic or semi-automatic detection. The task of determining intrinsic image points is difficult in different image modalities since the same points should be extracted in both images to be matched. Registering an image to physical space is very difficult or impossible using intrinsic point registration. Manual determination of intrinsic image points is very labor intensive and must be performed by a knowledgeable user. Finally, extrinsic point registration results can be visually verified by comparing the positions of the marker points in the images.

On the other hand, registration methods based on patient image properties have a number of advantages over extrinsic marker methods. Registration based on patient related image properties is fully retrospective. Since no special measures are necessary in the imaging protocol, the methods are very patient friendly. In contrast to temporary extrinsic marker methods, no special provisions are necessary if the studies to be registered are not done successively. Finally, patient related image properties may be used not only in rigid body transformations, but also in atlas methods (see Atlas Methods section).

Registration based on intrinsic or extrinsic fiducials is only accurate if the patient anatomy being imaged does not move during image acquisition. Thus it is extremely important to fix or immobilize the head during scanning.

Both intrinsic and extrinsic point registration methods frequently use rigid body transformations. The problem of estimating the translation and rotation parameters of the rigid body transformation that maps one space into another, given the coordinates of a number of corresponding points measured in the two coordinate systems, has been studied independently by researchers in psychology [31, 77, 95, 145, 166, 167], photogrammetry [71, 150, 168, 182], robotics [9, 51, 90, 91, 94], and statistics [75, 120, 169]. It was given the name "Orthogonal Procrustes" problem by Hurley and Cattell [95]; it is known as the "absolute orientation" problem in photogrammetry [71]. A closed-form solution was first discovered by Schönemann in 1966 [166]. Closed-form solutions using the singular value decomposition (SVD) of a matrix [9], the eigenvalue-eigenvector decomposition of a matrix [91], and unit quaternions [51, 90] have been independently rediscovered. Although some investigators have had success using iterative solution techniques [1, 60], a closed-form solution is clearly preferable.

Intrinsic point registration using rigid body transformations has been used to register CT and MR images for skull base surgery planning [86, 87, 88] and to register MR and PET images [45, 49]. Extrinsic point registration using rigid body transformations has been used to register CT, MR, and SPECT images to study the pathophysiology of cerebral infraction and hemorrhage [114] and to register CT and/or MR images with neuroelectromagnetic dipole data [14, 149, 151, 188, 190, 198] and neuromagnetic current density images [58]. The technique has also been used to register CT and/or MR images with physical space to

plan radiotherapy [81], use a stereotactic neurosurgical microscope [56, 163], and develop frameless stereotactic neurosurgical navigation systems [3, 60, 105, 116, 178].

One measure of registration accuracy is the distance between corresponding fiducials after registration. We call this accuracy measure *fiducial registration error*. A more important measure of registration accuracy is the distance between corresponding points other than those used to estimate the transformation parameters. Because such points might represent surgically targeted lesions, we call such points *targets* and the corresponding accuracy measure *target registration error*. Target registration error is a function of the number of fiducials used and the *fiducial localization error*, i.e. the error in determining the positions of the fiducials. Numerical simulations show that, for a fixed number of fiducials, the target registration error is roughly proportional to the fiducial localization error [2, 45, 47, 136]. For a fixed fiducial localization error, the target registration error is approximately inversely proportional to the square root of the number of fiducials used, e.g. quadrupling the number of fiducials used will approximately halve the target registration error. Intrinsic fiducial localization error, which is typically one to two voxels, is larger than extrinsic fiducial localization error, which is typically less than half of a voxel [140]. Thus registration using intrinsic fiducials requires using more points to achieve the equivalent accuracy obtained using extrinsic fiducials. One millimeter target registration error is theoretically possible when using four extrinsic fiducials, or about fifteen intrinsic fiducials, with 2 mm slice thickness image volumes [45, 47, 136].

Some point methods use polynomial warping functions to register images of deformable anatomy such as the abdomen and chest. Polynomial functions have been used to register serial myocardial perfusion projection images [171], pulmonary ventilation and perfusion projection images prior to subtraction [111], and CT and/or MR images with SPECT images of the abdomen [16, 117, 118, 119, 133, 134]. Other investigators have used intrinsic points to map atlases to images (see Atlas Methods section).

Curve and Surface Methods

These methods involve the determination of the coordinates of corresponding curves or surfaces in different images and the estimation of the geometric transformation using these corresponding structures. The curves or surfaces are derived from intrinsic structures, e.g. the inner surface of the skull in brain image volumes.

Balter et al. registered two-dimensional projection radiographs using manually digitized "open" curves [12]. Corresponding open curves were matched by searching for the optimal fit of the local curvatures in the two curves. The matched curves were then identically sampled in the overlapping segments to provide a set of corresponding points. The rigid body transformation was calculated using these points (see Point Methods section).

Gueziec and Ayache registered serial CT image volumes using three-dimensional curves [78, 181]. They automatically generate "ridge" or "crest" lines from derivatives of image intensity [143]. The discrete curves are approximated by a continuous spline to compute intrinsic differential features of second and third order, i.e. curvature and torsion. Corresponding curves are matched using a geometric hashing or "indexation" technique [112]. Basically, all of the curve points in one of the images are stored in a hash table which is indexed by curvature and torsion values. Curve points in the other image are compared with entries in the hash table and "votes" are accumulated for specific rigid body transformations.

Moshfeghi [144] extended an elastic matching algorithm developed by Burr [23] to use contour information to register images of deformable anatomy. The algorithm uses an iterative Gaussian smoothed deformation model. A displacement vector is calculated between each point in one contour and its nearest line segment from the other contour. One image is deformed by computing a displacement vector at every point in the image as a weighted average of its neighboring displacement vectors. This process is repeated a number of times, with decreasing elastic stiffness in each iteration to reduce the interacting neighborhood of the displacement vectors and allow matching of fine detail. The author used his technique to register two-dimensional CT and MR chest image slices.

Pelizzari, Chen, and colleagues developed a surface-based approach for registering multimodality brain image volumes [27, 153]. They fit a set of points ("hat") extracted from contours in one image to a surface model ("head") extracted from contours in the other image. The image that covers the larger volume of the patient, or the image that has a higher resolution if volume coverage is comparable, is used to generate the "head" surface model. A search technique due to Powell [157] is used to find the geometric transformation which, when applied to the "hat" coordinates, minimizes the mean squared distance between the "hat" points and the "head" surface. The distance between a "hat" point and the "head" surface is evaluated by finding the intersection with the "head" surface of a ray from the transformed "hat" point to the centroid of the "head" surface model. The intersections are found using a modification of a technique described by Siddon [170] which decomposes a three-dimensional line-volume intersection problem into a two-dimensional line-polygon intersection problem. The modification involves linear interpolation between the slices representing the "head" surface. The search involves some user interaction to circumvent the problem of local minima.

Several improvements on this increasingly popular registration technique are possible and have recently been reported. First, extraction of external contours is well suited to edge

detection methods and has been partially or fully automated by a number of investigators [96, 97, 146]. Second, many traditional search algorithms are thwarted by the presence of local minima which prevent the determination of the true global minimum. Neiw et al. used "simulated annealing" to reduce the problem of local minima [146]. Oghabian and Todd-Pokropek performed registration using a multiresolution pyramid technique to handle this problem [147]. They register the images using a series of surfaces extracted from the original images at different levels of resolution. The matching starts using the coarsest resolution surfaces, and the coarse resolution results are used to guide the registration at finer resolution levels. Finally, the time required to evaluate the goodness-of-fit metric can be significantly reduced by applying a distance transform to the surface extracted from one of the images. Barrow et al. originally described a technique using a distance transform to fit edge points from two images and efficiently computed the distance transform using a "chamfering" method [13]. Borgefors improved this "chamfer matching" technique and extended it by including a multiresolution pyramid approach [19]. Jiang et al. [96, 97] have implemented this technique in the commercially available medical imaging software package ANALYZE [160, 162]. Van den Elsen et al. have used hierarchical chamfer matching to register CT and MR images [185, 186]. They extract features using differential operators in scale space. Such mathematical operators may be used to extract geometrically invariant features from images [54]. They implemented their approach only in two dimensions, but it should be extensible to three dimensions.

Surface-based registration has been used clinically to register CT, MR, PET, and SPECT image volumes [89, 125, 126]. Recently the technique has been extended to include registration of image and physical space [127, 154]. This is accomplished by creating a surface map of the skin by sweeping it with a three-dimensional magnetic digitizer (Polhemus Navigation Science, Colchester, VT). One to two hundred surface points are acquired. This digitizer-derived surface is then registered to an image-derived surface using the surface matching algorithm.

The accuracy of surface-based registration has been investigated with phantom studies [153] and by expert (radiologist) examination of corresponding landmarks in patient head images [97]. It appears that registration accuracy is on the order of the voxel size.

Besl has recently published a promising shape registration algorithm which he calls the "iterative closest point" (ICP) algorithm [15]. The ICP algorithm can be used with the following geometric primitives: point sets, line segment sets, implicit curves, parametric curves, triangle sets, implicit surfaces, and parametric surfaces. Point sets are registered by means of one of the closed-form techniques developed for the Orthogonal Procrustes problem (see Point Methods section). All other cases are handled by iteratively assigning a point to each primitive, computing the transformation that registers the points, and applying that registration to the primitives themselves. The algorithm has not yet been applied to medical images.

Moment and Principal Axes Methods

The idea of matching images using moments is a fairly old idea due to Hu [93] and has been used in many non-medical applications, e.g. aircraft identification [42].

Moments are used in classical mechanics to characterize rigid bodies by the spatial distribution of their mass [177]. If a rigid body rotates, the components of its inertia tensor, relative to axes fixed in the body, do not change. The most convenient set of axes in the body are the principal axes of the inertia tensor, also called the principal axes of the body. The principal axes are those orthogonal axes about which the moments of inertia are minimized. If two objects are identical except for a translation and a rotation, then they can be registered exactly by bringing their principal axes into coincidence. If two objects are shaped similarly, they may be registered approximately by this process. Thus the general idea of the principal axes registration technique is to use the centroid of the points in image space as the origin and the eigenvectors of the covariance matrix of these points to specify the direction of the axes of the object reference system. The eigenvalues associated with these eigenvectors represent magnifications and may be used to specify scaling parameters.

Image volumes can be registered by means of the principal axes technique by using either corresponding "points" [10, 183], "surfaces" [62], or "volumes" [4, 8, 50]. Toennies et al. registered CT image volumes using corresponding points on the skull identified interactively using rendered images of the skull [183]. Alpert registered CT, MR, and PET images by manually determining the brain surface outline, image by image, to define a "volume of interest" which was treated as a rigid body with uniform mass density [4]. He suggests that using all of the volume elements in the "volume of interest" for registration is more accurate than using only the surface elements. He claims typical registration accuracies of 1 mm.

One major limitation of these techniques is that the results are very sensitive to missing image data. Accurate computation of the principal axes requires that the entire object be present in both image sets. Arata and Dhawan developed an iterative principal axes algorithm to minimize this sensitivity [8]. In each step, a transformation is computed using only object voxels contained in both image sets in the previous step. They register MR and PET images and show that their iterative algorithm is less sensitive to PET brain volume reduction due to a limited axial field of view than the standard algorithm. They state that they get accurate registration results when several contiguous slices are removed from the top of the cerebrum, but admit that even their improved technique is very sensitive to removal of just one slice from the base of the cerebellum.

Principal axes techniques are likely to be very sensitive to some pathological cases of probable interest to neurosurgeons, e.g. a large peripheral hypometabolic tumor in PET might cause a large MR-PET registration error. The applications of these methods are clearly limited to image-to-image registration.

Correlation Methods

Correlation methods attempt to determine the best registration maximizing the similarity between images of the same object that differ primarily because of different image acquisition conditions and also possibly because of small object changes. One first selects a parametized geometrical transformation to be applied to one of the images to correct for variations in acquisition conditions. The parameters of this transformation are then estimated by optimizing a similarity criterion between one image and the other transformed image.

The geometric transform can be rigid or non-rigid. Examples of rigid transformations can be found in [37, 152, 194, 200], which include only translation, and [38, 98], which include both translation and rotation. Translation and rotation are the elementary components of a rigid body transformation. In addition to rigid transformation, geometrical scaling is sometimes necessary for photographic views based on the use of a lens system because there is a direct relationship between the size of the object in the image and the distance between the object and the optical device. An intensity scaling is often important to correct for phenomena such as the differences in exposure times. In nuclear medicine, the intensity of a scintigraphic image is the result of the direct counting of the detected gamma photons. Thus an intensity scaling might be necessary to correct for the differences in acquisition times, injected activities, and backgrounds [195]. Examples that include rigid transformations plus some sort of scaling can be found in [6, 7], which include translation, rotation, and geometric scaling, and [85, 192, 195], which include translation, rotation, geometric scaling, and intensity scaling. To compensate for more complex image acquisition distortions or for non-rigid object motion, non-rigid transformations must be employed. Explorations of some non-rigid transformations include bilinear polynomial warping [53, 137]. higher degree polynomial warping [174, 191, 197], and exponential warping [199].

A justification for the use of geometrical image transformations to compensate for object motion is provided in [53]. There it is proved that subject to some mild restrictions easily realized for typical medical imaging situations, there always exists an image transformation that duplicates the effects of three-dimensional object motion. The restrictions, which require a calibration step, are that the images be maps of the density of some conserved quantity. A "conserved" quantity is one whose value within a region can be changed only by transport across the boundaries of the region. For non-medical applications such quantities are rare, but for medical imaging they are common. For example, in CT imaging the conserved quantity for a given tube voltage and filtering material is X-ray attenuation. In MR the conserved quantity for a given pulse sequence is the intensity of coherent, resonant radiation. In PET and SPECT for a given nuclide and activity level it is the intensity of gamma radiation. In addition to the tomographic modalities, the transformations exist for projection images, such as found in conventional X-ray imaging.

Several criteria of similarity or disparity have been proposed for calculating the values of the registration model parameters. Classical ones include the correlation function, the correlation coefficient, the sum of squares, and the sum of absolute values of differences. Several integer criteria have been somewhat recently proposed including sign change criteria [193].

The similarity criterion can be computed for every possible value of the registration parameters. This is rather computationally expensive. One group has used phase correlation

Fourier methods to estimate translation and rotation parameters [38]. Another group, which searched a space of bilinear geometric transforms to improve digital subtraction angiographic images of the coronary arteries, used genetic algorithms and simulated annealing to reduce the search time and the problem of local optima [137]. A more recent solution uses a cross-correlation technique employing Fourier invariance properties and logarithmic transforms to decouple the variables [6, 7].

Correlation methods are inherently useful primarily for monomodality image registration, particularly comparison of serial images of the same object, e.g. to look for small changes caused by disease. Good success has been obtained in registering serial medical photographs [192] and serial retinal angiographic images [152]. Correlation methods have also been used to stabilize images produced by a "digital television fundus camera" against random eye motion [37]. Junck et al. have reported using correlation methods to align functional brain image slices [98]. Although multimodality images usually contain complementary information, Apicella et al. register MR and PET image slices [6]. Rizzo et al. claim they can register CT, MR, PET, and SPECT image slices [159].

Interactive Methods

Pietrzyk et al. have recently developed a method to create corresponding brain slices from CT, MR, PET, and SPECT image volumes in individual patients [156]. Three-dimensional image registration is achieved by a variety of interactively controlled video display options. These include simultaneous display of multiple reformatted slices in all three dimensions for comparison of positioning. Brain contours in one imaging modality may be enhanced by appropriate filtering and superimposed onto reference images of another modality. They report reliable and reproducible registrations accurate to within about the distance corresponding to one voxel. They believe that this accuracy is due to the special capacity of the human visual system to analyze shapes and to detect systematic shifts of these shapes. In its present form, their method for functional-anatomical alignment can be employed only when the outer contours or other characteristic structures of the brain are clearly defined. Thus PET or SPECT images of tracers which are not distributed in considerable concentrations into the brain cortex cannot be used.

Kapouleas et al. developed a method which divides the three-dimensional MR-PET image registration problem into two two-dimensional problems [102, 103]. First the user aligns the interhemispheric fissure in the two volume images by specifying two of its points in each of several axial slices. Then the contours of each parasagittal slice in the MR image volume are overlaid on the corresponding PET image slice. A user interactively rotates and translates the MR image until the contours fit their counterparts on the PET image. The average of these rotations and translations combined with the partial transformation obtained in the first step constitutes the final registration transformation. In order to obtain reasonably good brain contours, high quality sagittal images are required. Sagittal views reformatted from transaxial images are usually not adequate. The authors claim a registration accuracy on the order of one to two voxels.

Ge et al. have developed a similar method by modifying the second step [63]. After aligning the interhemispheric fissure, equivalent points are identified by the user and the collection of paired points from multiple parasagittal reformatted slices are registered using a simple least squares minimization algorithm. They validated their method by using data obtained from clinical patients imaged with a stereotactic frame. They report a registration accuracy on the order of the size of one voxel.

These methods are retrospective and reasonably accurate. However, accurate use of these techniques requires that the user be familiar with the principles as well as the limitations peculiar to the applied imaging modalities. For example, Pietrzyk et al. note that brain structures with high levels of activity will always appear larger than neighboring structures with low levels of activity in functional images because of inherent blurring in the image acquisition process [156]. Thus asymmetric inactivation could result in a systemic shift of a functional image relative to an anatomic image when registering using their technique. A knowledgeable user could effectively control such a bias by determining a midline structure such as the interhemispheric fissure. The second step of the method of Ge et al. involves identification of equivalent points. This requires that the user be knowledgeable about the anatomy. The methods of both Kapouleas and Ge are probably very sensitive to deviations of the interhemispheric fissure from a planar configuration. All three of these methods are limited to image-to-image registration.

Atlas Methods

A logical extension of the image registration problem, especially for research studies, involves the registration of images from studies on separate individuals. This problem is more complex than the problem of registration within a given subject since variations in individual organ geometry must be taken into account. In the brain there is remarkable consistency of size and shape of anatomical structures between individuals provided that the image of the brain is scaled and oriented relative to deep internal structures. This observation has led to the construction of several anatomical atlases. A large number of investigators have recently reported work involving the registration of images and stereotactic anatomic atlases. The assumption underlying these methods is that at a certain level of representation, the topological structure of the brain is invariant among subjects. The objective then is to find the transformation that will map the atlas to the brain image, accounting for local shape differences in the process.

One approach is to establish a standard brain coordinate system. The Talairach proportional grid system is one such system which is widely used [179]. This system is based on the interhemispheric plane and the line passing through the top of the anterior commissure (AC) and the bottom of the posterior commissure (PC) in this plane. The AC-PC line has been shown to have a more constant relationship to key intracerebral structures than skull features or other brain landmarks [57, 179]. The plane passing through the AC-PC line perpendicular to the interhemispheric plane defines the horizontal plane. The plane passing through the posterior margin of the AC and perpendicular to the AC-PC line defines the vertical frontal plane. These two planes, plus the interhemispheric plane, make up an orthogonal coordinate system. The units along each axis of the coordinate system are proportionally established according to the maximum dimensions of the brain in the three planes. Registration based on the proportional grid system is essentially the determination of a piecewise affine transformation. Several groups have developed software to implement this system [46, 55, 57, 64, 124, 175]. There is a problem in establishing the proportional grid system on functional PET image volumes since the positions of the AC and PC cannot be directly determined. This problem has been solved by using a lateral skull radiograph [55] or by using other neighboring cerebral structures [57, 64].

The affine transformation used in the Talairach proportional grid system does not account for substantial nonlinearities in brain morphology, especially in cortical brain regions, among normal subjects, and this ultimately limits the use of that approach. A number of groups have developed registration techniques using nonlinear transformations.

Evans et al. constructed a three-dimensional computerized brain atlas by manually contouring 60 structures in each hemisphere on all slices of a high-resolution MR image volume [43, 44, 47, 139]. The contours for each structure were converted into a closed polyhedron using a tiling algorithm [28]. The atlas is deformed to fit the image data by interactive specification of homologous points in the atlas space and the image volume. The deformation is performed either with a global affine transformation or with the "thin-plate spline" warping function [18], which provides a well-behaved continuous space deformation between the specified landmark pairs. Distortion due to space-filling lesions can be dealt with by interactively editing surface points in the atlas to match the study image.

Greitz et al. constructed a computerized brain atlas by manually tracing approximately

250 structures on digitized photographs of one cryosectioned cadaver brain [17, 76]. The atlas is deformed to fit the study image volume in an interactive two-step process. First, the atlas is grossly positioned, oriented, and scaled by three-dimensional translation, rotation, and scaling transformations. Then the atlas is finely matched by deforming it with a series of two-dimensional second-degree polynomials. All transformation parameters are interactively specified.

Bajcsy, Dann, Gee, and colleagues developed a technique to elastically deform a three-dimensional computerized brain atlas to match CT and MR image volumes [11, 35, 36, 65, 66, 67]. The matching is implemented as a two-step process. First, the atlas and the study image volume are globally aligned using a principal axes method to remove translational, rotational, and scale differences. Then the atlas is elastically deformed to convert local shape differences in an iterative process that minimizes the sum of elastic deformation energy and image feature mismatch as estimated with a normalized cross correlation function. Essentially, the mapping matches the edges of the ventricles and the external surface of the brain; the resultant deformations are propagated throughout the atlas volume, deforming the remainder of the structures in the process. A coarse-to-fine multiresolution matching strategy is used to reduce computational complexity and increase registration accuracy. The authors specifically note that their approach is not designed to account for abnormal structures such as tumors, abscesses, strokes, and hemorrhages.

Atlas registration methods can be used to accumulate population statistics on morphologic variability in normals or disease states. The use of a standardized brain coordinate system has been used to signal-average functional image studies of sensory and cognitive activation [48, 180]. Atlas techniques may be useful in automatically segmenting individual cerebral structures in brain image volumes [32, 33]. Finally, these techniques may be useful in diagnosis and stereotactic neurosurgical planning [124].

Image Quality

Accurate three-dimensional image registration strongly depends on the quality of the image volumes. Because the head is essentially a rigid body, the best geometric transformation between volumetric head images and/or physical space would appear to be a rigid body transformation. Some investigators register images using an affine transformation to simultaneously estimate rigid body motion and correct for image distortion [1, 202]. However, the affine transformation may introduce distortions that are not really in the image, especially if a small number of features is being used for registration. Thus it is preferable that image distortions be avoided (by careful quality assurance) or corrected when possible before registration, and that registrations be performed using a rigid body transformation whenever feasible and appropriate. That is, the image distortion correction should be decoupled from the process of estimating the transformation parameters.

One possible problem can occur in images acquired with CT scanners in which the rotating X-ray source and detectors rotate in opposite directions in alternate slices (to prevent cables from coiling). If the forward and reverse starting angles are not in precise agreement, there will be apparent object rotation in alternate image slices. This problem is well known and is easily prevented by standard quality assurance studies. A block phantom should be routinely scanned and hardware and/or software adjustments made as necessary. Another possible problem in CT images occurs when the images are acquired with the gantry tilted obliquely relative to the direction of the table movement. If the volume image is constructed by simply "stacking" the image slices, then the volume is "sheared" or "skewed". The volume image is easily corrected if the slice thickness and gantry tilt angle are known. Henri et al. suggest determining the gantry tilt angle using fiducial markers in the images [84]. It is easier and more accurate to use the exact gantry tilt angle which is normally stored in the image file header.

A special concern arises with MR images because of geometrical distortions caused by static magnetic field inhomogeneity arising from imperfections in the magnet system or from magnetization of the object being imaged [129]. DeSoto et al. have developed an MR distortion model which can minimize distortions due to machine imperfections [40]. A special phantom is imaged and analyzed to determine the machine dependent parameters (an affine shear matrix) of the distortion model. These parameters are independent of time and pulse sequence. Two promising techniques for correcting distortions caused by magnetization of the object being imaged have recently been published. Chang and Fitzpatrick acquire two images of the same object with reversed gradients in the readout gradient direction and use these to produce a "rectified" image [24, 25, 26]. Sumanaweera et al. [176] have implemented an idea proposed by Feig et al. [52] which involves correcting distortion by extracting inhomogeneity information from the phase shifts of the image itself. The ultimate distortion correction probably involves using a combination of techniques that correct for machine dependent and object induced static magnetic field inhomogeneity.

These distortion corrections are not of vital interest in diagnostic radiology because radiologists are usually interested in the pattern and morphology of the image rather than in precise measurements. Precision measurements necessary for accurate registrations are of particular interest, however, to special disciplines such as stereotactic neurosurgery and stereotactic radiosurgery.

Summary

Registration techniques quantitatively relate the information in one image to information in another image by determining a one-to-one mapping between the points in each image. This makes it possible to superimpose features from one imaging study over those of another study. For example, skeletal structures and areas of contrast enhancement seen in CT images can be overlaid on MR images which clearly depict soft-tissue anatomy. Likewise, functional lesions detected with PET or SPECT can be viewed in the context of brain anatomy imaged with CT or MR. These methods can also be applied to multiple data sets obtained with the same modality at different times in order to bring the images into registration for the purpose of quantitative comparison, which increases the precision of treatment monitoring with serial images.

Registration techniques have recently been extended to relate image space to physical space. Stereotactic surgery and stereotactic radiosurgery require that an image or images be registered with the physical space occupied by the patient during surgery. An emerging interactive, image-guided surgery technology uses image-to-physical space registration to reflect the current surgical position on a display of the preoperative image sets of that patient.

Stereotactic frame systems generally include a stereotactic reference frame which provides rigid skull fixation using pins or screws and establishes a stereotactic coordinate system in physical space, a method for stereotactic image acquisition, and a system for mechanical direction of a probe or other surgical instrument to a defined intracranial point. Most current systems relate image space to the physical coordinate space established by the reference frame by attaching a localizing system consisting of N-shaped fiducials during image acquisition. Frame systems have several advantages: they are very accurate and they are immune to several types of image distortion, including geometric scaling and shearing due to gantry tilt. The primary disadvantages of frame systems are that they are somewhat difficult to learn to use, they cannot incorporate scans acquired before the frame was applied, they are somewhat cumbersome, and their use is limited to surgery since the fixation technique is invasive. Stereotactic frames are widely used for a large variety of applications, e.g. lesion biopsy, ventriculostomy, and radiosurgery. Neurosurgical planning software tools have been developed that allow neurosurgeons to correlate corresponding points in various images and to reconstruct oblique image slices to examine different biopsy trajectories. Stereotactic radiosurgery treatment planning systems have been reported that display isodose contours on images from various modalities. Frames have also been used to investigate the possibilities of interactive, image-guided surgery.

Point-based registration methods involve the determination of the coordinates of corresponding points in different images and/or physical space and the estimation of a geometric transformation using these corresponding points. The points may be either intrinsic, i.e. derived from patient specific properties, or extrinsic, i.e. derived from artificially applied markers. Registration based on patient related properties is fully retrospective. However, anatomic landmark selection is a labor intensive process. Further, it is difficult or impossible to register an image to physical space using intrinsic points. Registration using extrinsic points is not retrospective. However, any image modality and/or physical space can be registered as long as a marker can be constructed that is detectable. Extracting extrinsic marker

positions from medical images is often easier than extracting patient related image properties because the design of the markers can be optimized for automatic or semiautomatic detection. The registration results can be visually checked by comparing the positions of the marker points in the images. Anatomic landmarks have been used to register CT and MR images for skull base presurgical planning. Extrinsic markers have been used to register CT and/or MR images with physical space to plan radiotherapy, use a stereotactic neurosurgical microscope, and develop frameless stereotactic neurosurgical navigation systems.

A surface-based approach developed by Pelizzari, Chen, and colleagues registers images by fitting a set of points extracted from contours in one image to a surface model extracted from contours in the other image. This technique has been used clinically to register CT, MR, PET, and SPECT brain image volumes. Recently the technique has been extended to include registration of image and physical space by sweeping a three-dimensional magnetic digitizer across the skin to create a surface map of the skin. This digitizer-derived surface is then registered to an image-derived surface. This method is the only current registration technique that is both fully retrospective and able to register images to physical space. Registration results achieved with current implementations of this approach appear to be less accurate than those obtained with stereotactic frames systems and point-based methods. However, a great deal of effort is currently being spent improving surface-based registration.

Principal axes, correlation, and interactive registration methods are probably of limited value to neurosurgeons. None of these techniques can register images to physical space. The primary advantage of these methods is that they are fully retrospective. Principal axes methods register images by bringing the principal axes of the inertia tensors of corresponding objects in the images into coincidence. Registration accuracy is very sensitive to missing data since accurate computation of the principal axes requires that the entire object be present in both image sets. These techniques are likely also very sensitive to some pathological cases of probable interest to neurosurgeons, e.g. a large peripheral hypometabolic tumor in PET might cause a big MR-PET registration error. Correlation methods determine the transformation which optimizes a similarity criterion between one image and the other transformed image. These methods are inherently useful primarily for monomodality image registration, particularly comparison of serial images of the same object, e.g. to look for small changes caused by disease. Correlation techniques have mostly been used in medicine to register photographic and projection images, though a small number of researchers are currently investigating the registration of tomographic brain image slices. Interactive registration methods are time consuming and require knowledgeable users familiar with neuroanatomy and the principles as well as the limitations peculiar to the applied imaging modalities. It is also doubtful that they can obtain registration accuracy better than the dimension of one or two voxels.

A logical extension of the image registration problem, especially for research studies, involves the registration of images from studies on separate individuals. Anatomical atlases have been constructed based on the observation that in the brain there is a remarkable consistency of size and shape of anatomical structures between individuals provided that images of the brain are scaled and oriented relative to deep internal structures. A variety of methods have been developed to map atlases to brain images. Unfortunately, it is difficult to design an atlas which can account for abnormal structures such as tumors, abscesses, strokes, and hemorrhages. Nonetheless, atlas registration methods can be used to accumulate

population statistics on morphologic variability in normals or disease states, signal-average functional image studies of sensory and cognitive activation, and assist in automatically segmenting individual cerebral structures in brain image volumes. Atlas techniques might be useful to neurosurgeons for diagnosis and stereotactic neurosurgical planning.

Acknowledgements

The authors thank Yaorong Ge for helpful discussions and for providing many papers.

References

[1] A. B. Abche, G. S. Tzanakos, and E. Micheli-Tzanakou. A method for multimodal 3-D image registration with external markers. *Proc. Annu. Int. Conf. IEEE Eng. Med. Biol. Soc.*, 14:1881–1882, 1992.

[2] A. B. Abche, G. S. Tzanakos, and E. Micheli-Tzanakou. A Monte-Carlo evaluation of a multimodal 3-D image registration using external markers. *Proc. Annu. Int. Conf. IEEE Eng. Med. Biol. Soc.*, 14:1885–1887, 1992.

[3] L. Adams, W. Krybus, D. Meyer-Ebrecht, R. Rueger, J. M. Gilsbach, R. Moesges, and G. Schloendorff. Computer-assisted surgery. *IEEE Comput. Graphics Appl.*, 10:43–51, 1990.

[4] N. M. Alpert, J. F. Bradshaw, D. Kennedy, and J. A. Correia. The principal axes transformation: A method for image registration. *J. Nucl. Med.*, 31:1717–1722, 1990.

[5] S. L. Altmann. *Rotations, Quaternions, and Double Groups*. Oxford University Press, New York, 1986.

[6] A. Apicella, J. S. Kippenhan, and J. H. Nagel. Fast multi-modality image matching. *Medical Imaging III: Image Processing*, Proc. SPIE 1092:252–263, 1989.

[7] A. Apicella, J. H. Nagel, and R. Dura. Fast multimodality image matching. *Proc. Annu. Int. Conf. IEEE Eng. Med. Biol. Soc.*, 10:414–415, 1988.

[8] L. K. Arata and A. P. Dhawan. Iterative principal axes registration: A new algorithm for retrospective correlation of MR-PET brain images. *Proc. Annu. Int. Conf. IEEE Eng. Med. Biol. Soc.*, 14:2776–2778, 1992.

[9] K. S. Arun, T. S. Huang, and S. D. Blostein. Least-squares fitting of two 3-D point sets. *IEEE Trans. Pattern Anal. Mach. Intell.*, 9:698–700, 1987.

[10] R. Bajcsy and S. Kovacic. Multiresolution elastic matching. *Comput. Vision Graphics Image Processing*, 46:1–21, 1989.

[11] R. Bajcsy, R. Lieberson, and M. Reivich. A computerized system for the elastic matching of deformed radiographic images to idealized atlas images. *J. Comput. Assist. Tomogr.*, 7:618–625, 1983.

[12] J. M. Balter, C. A. Pelizzari, and G. T. Y. Chen. Correlation of projection radiographs in radiation therapy using open curve segments and points. *Med. Phys.*, 19:329–334, 1992.

[13] H. G. Barrow, J. M. Tenenbaum, R. C. Bolles, and H. C. Wolf. Parametric correspondence and chamfer matching: Two new techniques for image matching. *Proc. 5th Int. Joint Conf. Artificial Intelligence*, pages 659–663, 1977.

[14] D. S. Barth, W. Sutherling, J. Engle, Jr., and J. Beatty. Neuromagnetic evidence of spatially distributed sources underlying epileptiform spikes in the human brain. *Science*, 223:293–296, 1984.

[15] P. J. Besl and N. D. McKay. A method for registration of 3-D shapes. *IEEE Trans. Pattern Anal. Mach. Intell.*, 14:239–256, 1992.

[16] B. A. Birnbaum, M. E. Noz, J. Chapnick, J. J. Sanger, A. J. Megibow, G. Q. Maguire, Jr., J. C. Weinreb, E. M. Kaminer, and E. L. Kramer. Hepatic hemangiomas: Diagnosis with fusion of MR, CT, and Tc-99m-labeled red blood cell SPECT images. *Radiology*, 181:469–474, 1991.

[17] C. Bohm, T. Greitz, R. Seitz, and L. Eriksson. Specification and selection of regions of interest (ROIs) in a computerized brain atlas. *J. Cereb. Blood Flow Metab.*, 11:A64–A68, 1991.

[18] F. L. Bookstein. Principal warps: Thin-plate splines and the decomposition of deformations. *IEEE Trans. Pattern Anal. Mach. Intell.*, 11:567–585, 1989.

[19] G. Borgefors. Hierarchical chamfer matching: A parametric edge matching algorithm. *IEEE Trans. Pattern Anal. Mach. Intell.*, 10:849–865, 1988.

[20] R. A. Brown. A computerized tomography-computer graphics approach to stereotaxic localization. *J. Neurosurg.*, 50:715–720, 1979.

[21] R. A. Brown. A stereotactic head frame for use with CT body scanners. *Invest. Radiol.*, 14:300–304, 1979.

[22] R. A. Brown, T. S. Roberts, and A. G. Osborn. Stereotaxic frame and computer software for CT-directed neurosurgical localization. *Invest. Radiol.*, 15:308–312, 1980.

[23] D. J. Burr. A dynamic model for image registration. *Comput. Vision Graphics Image Processing*, 15:102–112, 1981.

[24] H. Chang. *Geometrical Image Transformation to Compensate for Distortion in Magnetic Resonance Imaging.* PhD thesis, Vanderbilt University, Nashville, TN, 1990.

[25] H. Chang and J. M. Fitzpatrick. Geometric image transformation to compensate for MRI distortions. *Medical Imaging IV: Image Processing*, Proc. SPIE 1233:116–127, 1990.

[26] H. Chang and J. M. Fitzpatrick. A technique for accurate magnetic resonance imaging in the presence of field inhomogeneities. *IEEE Trans. Med. Imaging*, 11:319–329, 1992.

[27] C.-T. Chen, C. A. Pelizzari, G. T. Y. Chen, M. D. Cooper, and D. N. Levin. Image analysis of PET data with the aid of CT and MR images. In C. N. de Graaf and M. A. Viergever, editors, *Information Processing in Medical Imaging 1987*, pages 601–611. Plenum Press, New York, 1988.

[28] H. N. Christiansen and T. W. Sederberg. Conversion of complex contour line definitions into polygonal element mosaics. *Comput. Graphics*, 12:187–192, 1978.

[29] R. H. Clarke and V. Horsley. On a method of investigating the deep ganglia and tracts of the central nervous system (cerebellum). *Br. Med. J.*, 2:1799–1800, 1906.

[30] P. Clarysse, D. Gibon, J. Rousseau, S. Blond, C. Vasseur, and X. Marchandise. A computer-assisted system for 3-D frameless localization in stereotaxic MRI. *IEEE Trans. Med. Imaging*, 10:523–529, 1991.

[31] N. Cliff. Orthogonal rotation to congruence. *Psychometrika*, 31:33–42, 1966.

[32] D. L. Collins, T. M. Peters, W. Dai, and A. C. Evans. Model based segmentation of individual brain structures from MRI data. *Visualization in Biomedical Computing 1992*, Proc. SPIE 1808:10–23, 1992.

[33] D. L. Collins, T. M. Peters, and A. C. Evans. Multiresolution image registration and brain structure segmentation. In C. Roux, G. T. Herman, and R. Collorec, editors, *3D Advanced Image Processing in Medicine 1992*, pages 105–109, 1992.

[34] J. Conti, M. D. F. Deck, and D. A. Rottenberg. An inexpensive video patient repositioning system for use with transmission and emission computed tomographs. *J. Comput. Assist. Tomogr.*, 6:417–421, 1982.

[35] R. Dann, J. Hoford, S. Kovacic, M. Reivich, and R. Bajcsy. Three-dimensional computerized brain atlas for elastic matching: Creation, and initial evaluation. *Medical Imaging II: Image Formation, Detection, Processing, and Interpretation*, Proc. SPIE 914:600–608, 1988.

[36] R. Dann, J. Hoford, S. Kovacic, M. Reivich, and R. Bajcsy. Evaluation of elastic matching system for anatomic (CT, MR) and functional (PET) cerebral images. *J. Comput. Assist. Tomogr.*, 13:603–611, 1989.

[37] E. De Castro, G. Cristini, A. Martelli, C. Morandi, and M. Vascotto. Compensation of random eye motion in television ophthalmoscopy: Preliminary results. *IEEE Trans. Med. Imaging*, 6:74–81, 1987.

[38] E. De Castro and C. Morandi. Registration of translated and rotated images using finite Fourier transforms. *IEEE Trans. Pattern Anal. Mach. Intell.*, 9:700–703, 1987.

[39] L. A. DeSoto, H. S. Choi, D. R. Haynor, Y. Kim, K. J. Burchiel, and T. S. Roberts. Multiplanar imaging system for stereotaxic neurosurgery. *Medical Imaging III: Image Capture and Display*, Proc. SPIE 1091:31–41, 1989.

[40] L. A. DeSoto, D. R. Haynor, and Y. Kim. Three-dimensional distortion model for magnetic resonance images. *Medical Imaging VI: Image Capture, Formatting, and Display*, Proc. SPIE 1653:?–?, 1992.

[41] C. Dittmar. Über die lage des sogenannten gefäfsszentrums in der medulla oblongata. *Ber Saechs Ges Wiss Leipzig (Math Phys)*, 25:449–469, 1873.

[42] S. A. Dudani, K. J. Breeding, and R. B. McGhee. Aircraft identification by moment invariants. *IEEE Trans. Comput.*, 26:39–45, 1977.

[43] A. C. Evans, C. Beil, S. Marrett, C. J. Thompson, and A. Hakim. Anatomical-functional correlation using an adjustable MRI-based region of interest atlas with positron emission tomography. *J. Cereb. Blood Flow Metab.*, 8:513–530, 1988.

[44] A. C. Evans, W. Dai, D. L. Collins, P. Neelin, and S. Marrett. Warping of a computerized 3-D atlas to match brain image volumes for quantitative neuroanatomical and functional analysis. *Medical Imaging V: Image Processing*, Proc. SPIE 1445:236–246, 1991.

[45] A. C. Evans, S. Marrett, D. L. Collins, and T. M. Peters. Anatomical-functional correlative analysis of the human brain using three dimensional imaging systems. *Medical Imaging III: Image Processing*, Proc. SPIE 1092:264–274, 1989.

[46] A. C. Evans, S. Marrett, P. Neelin, D. L. Collins, K. Worsley, W. Dai, S. Milot, E. Meyer, and D. Bub. Anatomical mapping of functional activation in stereotactic coordinate space. *Neuroimage*, 1:43–53, 1992.

[47] A. C. Evans, S. Marrett, J. Torrescorzo, S. Ku, and D. L. Collins. MRI-PET correlation in three dimensions using a volume-of-interest (VOI) atlas. *J. Cereb. Blood Flow Metab.*, 11:A69–A78, 1991.

[48] A. C. Evans, P. Neelin, S. Marrett, E. Meyer, W. Dai, and D. L. Collins. Combined stereotactic mapping of MRI and PET studies of cognitive activation in human brain. *Proc. Annu. Int. Conf. IEEE Eng. Med. Biol. Soc.*, 13:224–226, 1991.

[49] A. C. Evans, T. M. Peters, D. L. Collins, C. J. Henri, S. Marrett, G. B. Pike, and W. Dai. 3-D correlative imaging and segmentation of cerebral anatomy, function and vasculature. *Automedica*, 14:65–80, 1992.

[50] T. L. Faber and E. M. Stokely. Orientation of 3-D structures in medical images. *IEEE Trans. Pattern Anal. Mach. Intell.*, 10:626–633, 1988.

[51] O. D. Faugeras and M. Hebert. The representation, recognition, and locating of 3-D objects. *Int. J. Robotics Res.*, 5:27–52, 1986.

[52] E. Feig, F. Greenleaf, and M. Perlin. Magnetic resonance imaging with non-uniform fields. *Phys. Med. Biol.*, 31:1091–1099, 1986.

[53] J. M. Fitzpatrick, D. R. Pickens, III, J. J. Grefenstette, R. P. Price, and A. E. James, Jr. Technique for automatic motion correction in digital subtraction angiography. *Opt. Eng.*, 26:1085–1093, 1987.

[54] L. M. J. Florack, B. M. ter Haar Romeny, J. J. Koenderink, and M. A. Viergever. Scale and the differential structure of images. *Image Vision Comput.*, 10:376–388, 1992.

[55] P. T. Fox, J. S. Perlmutter, and M. E. Raichle. A stereotactic method of anatomical localization for positron emission tomography. *J. Comput. Assist. Tomogr.*, 9:141–153, 1985.

[56] E. M. Friets, J. W. Strohbehn, J. F. Hatch, and D. W. Roberts. A frameless stereotaxic operating microscope for neurosurgery. *IEEE Trans. Biomed. Eng.*, 36:608–617, 1989.

[57] K. J. Friston, R. E. Passingham, J. G. Nutt, J. D. Heather, G. V. Sawle, and R. S. J. Frackowiak. Localization in PET images: Direct fitting of the intercommissural (AC-PC) line. *J. Cereb. Blood Flow Metab.*, 9:690–695, 1989.

[58] M. Fuchs, H.-A. Wischmann, and O. Dössel. Overlay of neuromagnetic current density images and morphological MR images. *Visualization in Biomedical Computing 1992*, Proc. SPIE 1808:676–684, 1992.

[59] R. L. Galloway, Jr. and R. J. Maciunas. Stereotactic neurosurgery. *Crit. Rev. Biomed. Eng.*, 18:207–233, 1990.

[60] R. L. Galloway, Jr., R. J. Maciunas, and C. A. Edwards, II. Interactive image-guided neurosurgery. *IEEE Trans. Biomed. Eng.*, 39:1226–1231, 1992.

[61] R. L. Galloway, Jr., R. J. Maciunas, and J. W. Latimer. The accuracies of four stereotactic frame systems: An independent assessment. *Biomed. Instrum. Technol.*, 25:457–460, 1991.

[62] A. Gamboa-Aldeco, L. L. Fellingham, and G. T. Y. Chen. Correlation of 3D surfaces from multiple modalities in medical imaging. *Medicine XIV/PACS IV*, Proc. SPIE 626:467–473, 1986.

[63] Y. Ge, J. M. Fitzpatrick, J. R. Votaw, S. Gadamsetty, R. J. Maciunas, R. M. Kessler, and R. A. Margolin. Retrospective registration of PET and MR brain images: An algorithm and its stereotactic validation. Submitted 1993.

[64] Y. Ge, J. R. Votaw, R. A. Margolin, J. M. Fitzpatrick, R. J. Maciunas, and R. M. Kessler. Reformatting PET images by direct fitting of the proportional grid system: Implementation and validation. *Medical Imaging VI: Image Processing*, Proc. SPIE 1652:397–408, 1992.

[65] J. C. Gee, M. Reivich, and R. Bajcsy. Quantitative analysis of cerebral images using an elastically deformable atlas: theory and validation. *Medical Imaging VI: Image Processing*, Proc. SPIE 1652:260–270, 1992.

[66] J. C. Gee, M. Reivich, and R. Bajcsy. Elastically deforming a three-dimensional atlas to match anatomical brain images. *J. Comput. Assist. Tomogr.*, 17:225–236, 1993.

[67] J. C. Gee, M. Reivich, L. Bilaniuk, D. Hackney, R. Zimmerman, S. Kovacic, and R. Bajcsy. Evaluation of multiresolution elastic matching using MRI data. *Medical Imaging V: Image Processing*, Proc. SPIE 1445:226–234, 1991.

[68] P. Gerlot and Y. Bizais. Image registration: A review and a strategy for medical applications. In C. N. de Graaf and M. A. Viergever, editors, *Information Processing in Medical Imaging 1987*, pages 81–89. Plenum Press, New York, 1988.

[69] P. Gerlot-Chiron and Y. Bizais. Definition and evaluation of a surface overlap criterion for medical image registration. In D. A. Ortendahl and J. Llacer, editors, *Information Processing in Medical Imaging 1989*, pages 429–442. Wiley-Liss, New York, 1991.

[70] P. Gerlot-Chiron and Y. Bizais. Registration of multimodality medical images using a region overlap criterion. *CVGIP: Graphical Models and Image Processing*, 54:396–406, 1992.

[71] S. K. Ghosh. *Analytical Photogrammetry.* Pergamon Press, New York, 2nd edition, 1988.

[72] S. J. Goerss, P. J. Kelly, B. A. Kall, and G. J. Alker, Jr. A computed tomographic stereotactic adaptation system. *Neurosurgery*, 10:375–379, 1982.

[73] A. Goshtasby. Piecewise linear mapping functions for image registration. *Pattern Recognition*, 19:459–466, 1986.

[74] A. Goshtasby. Piecewise cubic mapping functions for image registration. *Pattern Recognition*, 20:525–533, 1987.

[75] J. C. Gower. Statistical methods of comparing different multivariate analyses of the same data. In F. R. Hodson, D. G. Kendall, and P. Tautu, editors, *Mathematics in the Archaeological and Historical Sciences*, pages 138–149. Edinburgh University Press, Edinburgh, 1975.

[76] T. Greitz, C. Bohm, S. Holte, and L. Eriksson. A computerized brain atlas: Construction, anatomical content, and some applications. *J. Comput. Assist. Tomogr.*, 15:26–38, 1991.

[77] G. T. Gruvaeus. A general approach to Procrustes pattern rotation. *Psychometrika*, 35:493–505, 1970.

[78] A. Gueziec and N. Ayache. Smoothing and matching of 3-D space curves. *Visualization in Biomedical Computing 1992*, Proc. SPIE 1808:259–273, 1992.

[79] D. J. Hawkes, D. L. G. Hill, and E. E. C. M. L. Bracey. Multi-modal data fusion to combine anatomical and physiological information in the head and heart. In J. H. C. Reiber and E. E. van der Wall, editors, *Cardiovascular Nuclear Medicine and MRI: Quantitation and Clinical Applications*, pages 113–130. Kluwer Academic Publishers, Dordrecht, 1992.

[80] D. J. Hawkes, D. L. G. Hill, E. D. Lehmann, G. P. Robinson, M. N. Maisey, and A. C. F. Colchester. Preliminary work on the interpretation of SPECT images with the aid of registered MR images and an MR derived 3D neuro-anatomical atlas. In K. H. Höhne, H. Fuchs, and S. M. Pizer, editors, *3D Imaging in Medicine: Algorithms, Systems, Applications*, pages 241–252. Springer-Verlag, Berlin, 1990.

[81] D. R. Haynor, A. W. Borning, B. A. Griffin, J. P. Jacky, I. J. Kalet, and W. P. Shuman. Radiotherapy planning: Direct tumor location on simulation and port films using CT. *Radiology*, 158:537–540, 1986.

[82] M. P. Heilbrun, editor. *Stereotactic Neurosurgery.* Williams & Wilkins, Baltimore, 1988.

[83] M. P. Heilbrun, P. M. Sunderland, P. R. McDonald, T. H. Wells, Jr., E. Cosman, and E. Ganz. Brown-Roberts-Wells stereotactic frame modifications to accomplish magnetic resonance imaging guidance in three planes. *Appl. Neurophysiol.*, 50:143–152, 1987.

[84] C. J. Henri, D. L. Collins, T. M. Peters, A. C. Evans, and S. Marrett. Three-dimensional interactive display of medical images for stereotactic neurosurgery planning. *Medical Imaging III: Image Processing*, Proc. SPIE 1092:67–74, 1989.

[85] M. Herbin, A. Venot, J. Y. Devaux, E. Walter, J. F. Lebruchec, L. Dubertret, and J. C. Roucayrol. Automated registration of dissimilar images: Application to medical imagery. *Comput. Vision Graphics Image Processing*, 47:77–88, 1989.

[86] D. L. G. Hill, S. E. M. Green, J. E. Crossman, D. J. Hawkes, G. P. Robinson, C. F. Ruff, T. C. S. Cox, A. J. Strong, and M. J. Gleeson. Visualisation of multi-modal images for the planning of skull base surgery. *Visualization in Biomedical Computing 1992*, Proc. SPIE 1808:564–573, 1992.

[87] D. L. G. Hill, D. J. Hawkes, J. E. Crossman, M. J. Gleeson, T. C. S. Cox, E. E. C. M. L. Bracey, A. J. Strong, and P. Graves. Registration of MR and CT images for skull base surgery using point-like anatomical features. *Br. J. Radiol.*, 64:1030–1035, 1991.

[88] D. L. G. Hill, D. J. Hawkes, Z. Hussain, S. E. M. Green, C. F. Ruff, and G. P. Robinson. Accurate combination of CT and MR data of the head: Validation and applications in surgical and therapy planning. In C. Roux, G. T. Herman, and R. Collorec, editors, *3D Advanced Image Processing in Medicine 1992*, pages 79–83, 1992.

[89] B. L. Holman, R. E. Zimmerman, K. A. Johnson, P. A. Carvalho, R. B. Schwartz, J. S. Loeffler, E. Alexander, C. A. Pelizzari, and G. T. Y. Chen. Computer-assisted superimposition of magnetic resonance and high-resolution technetium-99m-HMPAO and thallium-201 SPECT images of the brain. *J. Nucl. Med.*, 32:1478–1484, 1991.

[90] B. K. P. Horn. Closed-form solution of absolute orientation using unit quaternions. *J. Opt. Soc. Amer. A*, 4:629–642, 1987.

[91] B. K. P. Horn, H. M. Hilden, and S. Negahdaripour. Closed-form solution of absolute orientation using orthonormal matrices. *J. Opt. Soc. Amer. A*, 5:1127–1135, 1988.

[92] V. Horsley and R. H. Clarke. The structure and function of the cerebellum examined by a new method. *Brain*, 31:45–124, 1908.

[93] M. K. Hu. Visual pattern recognition by moment invariants. *IEEE Trans. Inform. Theory*, 8:179–187, 1962.

[94] T. S. Huang, S. D. Blostein, and E. A. Margerum. Least-squares estimation of motion parameters from 3-D point correspondences. *Proc. IEEE Conf. Comput. Vision Pattern Recognition*, pages 198–200, 1986.

[95] J. R. Hurley and R. B. Cattell. The Procrustes program: Producing direct rotation to test a hypothesized factor structure. *Behav. Sci.*, 7:258–262, 1962.

[96] H. Jiang, K. S. Holton, and R. A. Robb. Image registration of multimodality 3-D medical images by chamfer matching. *Biomedical Image Processing and Three-Dimensional Microscopy 1992*, Proc. SPIE 1660:356–366, 1992.

[97] H. Jiang, R. A. Robb, and K. S. Holton. A new approach to 3-D registration of multimodality medical images by surface matching. *Visualization in Biomedical Computing 1992*, Proc. SPIE 1808:196–213, 1992.

[98] L. Junck, J. G. Moen, G. D. Hutchins, M. B. Brown, and D. E. Kuhl. Correlation methods for the centering, rotation, and alignment of functional brain images. *J. Nucl. Med.*, 31:1220–1226, 1990.

[99] B. A. Kall, P. J. Kelly, and S. J. Goerss. Comprehensive computer-assisted data collection treatment planning and interactive surgery. *Medical Imaging*, Proc. SPIE 767:509–514, 1987.

[100] E. I. Kandel. Stereotaxic apparatus and operations in russia in the 19th century. *J. Neurosurg.*, 37:407–411, 1972.

[101] E. I. Kandel. *Functional and Stereotactic Neurosurgery.* Plenum Medical Book Company, New York, 1989.

[102] I. Kapouleas. Error analysis of 3D registration of brain MR and PET images using the interhemispheric fissure. *Proc. Annu. Int. Conf. IEEE Eng. Med. Biol. Soc.*, 13:227–228, 1991.

[103] I. Kapouleas, A. Alavi, W. M. Alves, R. E. Gur, and D. W. Weiss. Registration of three-dimensional MR and PET images of the human brain without markers. *Radiology*, 181:731–739, 1991.

[104] J. N. Kapur, P. K. Sahoo, and A. K. C. Wong. A new method for gray-level picture thresholding using the entropy of the histogram. *Comput. Vision Graphics Image Processing*, 29:273–285, 1985.

[105] A. Kato, T. Yoshimine, T. Hayakawa, Y. Tomita, T. Ikeda, M. Mitomo, K. Harada, and H. Mogami. A frameless, armless navigational system for computer-assisted tomography. *J. Neurosurg.*, 74:845–849, 1991.

[106] K. J. Kearfott, D. A. Rottenberg, and R. J. R. Knowles. A new headholder for PET, CT, and NMR imaging. *J. Comput. Assist. Tomogr.*, 8:1217–1220, 1984.

[107] P. J. Kelly. Principles of stereotactic surgery. In J. R. Youmans, editor, *Neurological Surgery: A Comprehensive Reference Guide to the Diagnosis and Management of Neurosurgical Problems, 3rd edition*, pages 4183–4226. W. B. Saunders Company, Philadelphia, 1990.

[108] P. J. Kelly. *Tumor Stereotaxis*. W. B. Saunders Company, Philadelphia, 1991.

[109] P. J. Kelly, B. A. Kall, and S. J. Goerss. Computer simulation for the stereotactic placement of interstitial radionuclide sources into computed tomography defined tumor volumes: Technical note. *Neurosurgery*, 14:442–448, 1984.

[110] P. J. Kelly, B. A. Kall, and S. J. Goerss. Transposition of volumetric information derived from computed tomography scanning into stereotactic space. *Surg. Neurol.*, 21:465–471, 1984.

[111] P. A. Kenny, D. J. Dowsett, D. Vernon, and J. T. Ennis. A technique for digital image registration used prior to subtraction of lung images in nuclear medicine. *Phys. Med. Biol.*, 35:679–685, 1990.

[112] E. Kishon, T. Hastie, and H. Wolfson. 3-D curve matching using splines. Technical report, AT&T, November 1989.

[113] J. Kittler, J. Illingworth, and J. Föglein. Threshold selection based on a simple image statistic. *Comput. Vision Graphics Image Processing*, 30:125–147, 1985.

[114] N. M. J. Knufman, P. A. Van den Elsen, J. P. M. Cillessen, J. W. Van Isselt, and C. A. F. Tulleken. Spatial integration of multimodal brain images in cerebral infarction. *Brain Topogr.*, 5:165–170, 1992.

[115] M. Koslow, M. G. Abele, R. C. Griffith, G. A. Mair, and N. E. Chase. Stereotactic surgical system controlled by computed tomography. *Neurosurgery*, 8:72–82, 1981.

[116] Y. Kosugi, E. Watanabe, J. Goto, T. Watanabe, S. Yoshimoto, K. Takakura, and J. Ikebe. An articulated neurosurgical navigation system using MRI and CT images. *IEEE Trans. Biomed. Eng.*, 35:147–152, 1988.

[117] E. L. Kramer and M. E. Noz. CT-SPECT fusion for analysis of radiolabeled antibodies: Applications in gastrointestinal and lung carcinoma. *Nucl. Med. Biol.*, 18:27–42, 1991.

[118] E. L. Kramer, M. E. Noz, G. Q. Maguire, Jr., J. J. Sanger, C. Walsh, and E. Millan. Fusing of immunoscintigraphy SPECT with CT or MRI for improved multimodality image interpretation. *Proc. Annu. Int. Conf. IEEE Eng. Med. Biol. Soc.*, 14:1805–1806, 1992.

[119] E. L. Kramer, M. E. Noz, J. J. Sanger, A. J. Megibow, and G. Q. Maguire, Jr. CT-SPECT fusion to correlate radiolabeled monoclonal antibody uptake with abdominal CT findings. *Radiology*, 172:861–865, 1989.

[120] W. J. Krzanowski. A comparison of some distance measures applicable to multinomial data, using a rotational fit technique. *Biometrics*, 27:1062–1068, 1971.

[121] L. Leksell, T. Herner, D. Leksell, B. Persson, and C. Lindquist. Visualisation of stereotactic radiolesions by nuclear magnetic resonance. *J. Neurol. Neurosurg. Psychiatry*, 48:19–20, 1985.

[122] L. Leksell and B. Jernberg. Stereotaxis and tomography: A technical note. *Acta Neurochir.*, 52:1–7, 1980.

[123] L. Leksell, D. Leksell, and J. Schwebel. Stereotaxic and nuclear magnetic resonance. *J. Neurol. Neurosurg. Psychiatry*, 48:14–18, 1985.

[124] D. Lemoine, C. Barillot, B. Gibaud, and E. Pasqualini. An anatomical-based 3D registration system of multimodality and atlas data in neurosurgery. In A. C. F. Colchester and D. J. Hawkes, editors, *Information Processing in Medical Imaging 1991*, pages 154–164. Springer-Verlag, Berlin, 1991.

[125] D. N. Levin, X. Hu, K. K. Tan, S. Galhotra, C. A. Pelizzari, G. T. Y. Chen, R. N. Beck, C.-T. Chen, M. D. Cooper, J. F. Mullan, J. Hekmatpanah, and J.-P. Spire. The brain: Integrated three-dimensional display of MR and PET images. *Radiology*, 172:783–789, 1989.

[126] D. N. Levin, C. A. Pelizzari, G. T. Y. Chen, C.-T. Chen, and M. D. Cooper. Retrospective geometric correlation of MR, CT, and PET images. *Radiology*, 169:817–823, 1988.

[127] D. N. Levin, K. K. Tan, C. A. Pelizzari, R. Grzeszczuk, G. T. Y. Chen, G. J. Dohrmann, and R. K. Erickson. Computer-assisted treatment of brain lesions with the aid of 3-D images. *Proc. Annu. Int. Conf. IEEE Eng. Med. Biol. Soc.*, 13:1329–1330, 1991.

[128] J. T. Lewis and R. L. Galloway, Jr. Ultrasonic detection of subcutaneous fiducial markers for image-physical space registration. *Proc. Annu. Int. Conf. IEEE Eng. Med. Biol. Soc.*, 14:1061–1062, 1992.

[129] K. M. Lüdeke, P. Röschmann, and R. Tischler. Susceptibility artifacts in NMR imaging. *Magn. Reson. Imaging*, 3:329–343, 1985.

[130] L. D. Lunsford, A. J. Martinez, and R. E. Latchaw. Stereotaxic surgery with a magnetic resonance- and computerized tomography-compatible system. *J. Neurosurg.*, 64:872–878, 1986.

[131] R. J. Maciunas, R. L. Galloway, Jr., J. Latimer, C. Cobb, E. Zaccharias, A. Moore, and V. R. Mandava. An independent application accuracy evaluation of stereotactic frame systems. *Stereotactic Funct. Neurosurg.*, 58:103–107, 1992.

[132] R. J. Maciunas, R. M. Kessler, C. R. Maurer, Jr., V. R. Mandava, G. Watt, and G. Smith. Positron emission tomography imaging-directed stereotactic neurosurgery. *Stereotactic Funct. Neurosurg.*, 58:134–140, 1992.

[133] G. Q. Maguire, Jr., M. E. Noz, E. M. Lee, and J. H. Schimpf. Correlation methods for tomographic images using two and three dimensional techniques. In S. L. Bacharach, editor, *Information Processing in Medical Imaging 1985*, pages 266–279. Martinus Nijhoff Publishers, Dordrecht, 1986.

[134] G. Q. Maguire, Jr., M. E. Noz, H. Rusinek, J. Jaeger, E. L. Kramer, J. J. Sanger, and G. Smith. Graphics applied to medical image registration. *IEEE Comput. Graphics Appl.*, 11:20–29, March 1991.

[135] V. R. Mandava. *Three Dimensional Multimodal Image Registration Using Implanted Markers*. PhD thesis, Vanderbilt University, Nashville, TN, 1991.

[136] V. R. Mandava, J. M. Fitzpatrick, C. R. Maurer, Jr., R. J. Maciunas, and G. S. Allen. Registration of multimodal volume head images via attached markers. *Medical Imaging VI: Image Processing*, Proc. SPIE 1652:271–282, 1992.

[137] V. R. Mandava, J. M. Fitzpatrick, and D. R. Pickens, III. Adaptive search space scaling in digital image registration. *IEEE Trans. Med. Imaging*, 8:251–262, 1989.

[138] V. R. Mandava, R. J. Maciunas, J. M. Fitzpatrick, R. L. Galloway, Jr., and C. R. Maurer, Jr. A workstation platform for stereotactic neurosurgical planning. *Proc. Annu. Int. Conf. IEEE Eng. Med. Biol. Soc.*, 13:1220–1221, 1991.

[139] S. Marrett, A. C. Evans, L. Collins, and T. M. Peters. A volume of interest (VOI) atlas for the analysis of neurophysiological image data. *Medical Imaging III: Image Processing*, Proc. SPIE 1092:467–477, 1989.

[140] C. R. Maurer, Jr., J. J. McCrory, and J. M. Fitzpatrick. Estimation of accuracy in localizing externally attached markers in multimodal volume head images. *Medical Imaging VII: Image Processing*, Proc. SPIE 1898:43–54, 1993.

[141] J. C. Mazziotta, M. E. Phelps, A. K. Meadors, A. Ricci, J. Winter, and J. R. Bentson. Anatomical localization schemes for use in positron computed tomography using a specially designed headholder. *J. Comput. Assist. Tomogr.*, 6:848–853, 1982.

[142] C. C. Meltzer, R. N. Bryan, H. H. Holcomb, A. W. Kimball, H. S. Mayberg, B. Sadzot, J. P. Leal, H. N. Wagner, Jr., and J. J. Frost. Anatomical localization for PET using MR imaging. *J. Comput. Assist. Tomogr.*, 14:418–426, 1990.

[143] O. Monga, S. Benayoun, and O. D. Faugeras. From partial derivatives of 3D density images to ridge lines. *Visualization in Biomedical Computing 1992*, Proc. SPIE 1808:118–129, 1992.

[144] M. Moshfeghi. Elastic matching of multimodality medical images. *CVGIP: Graphical Models and Image Processing*, 53:271–282, 1991.

[145] C. I. Mosier. Determining a simple structure when loadings for certain tests are known. *Psychometrika*, 4:149–162, 1939.

[146] H. M. Neiw, C.-T. Chen, W. C. Lin, and C. A. Pelizzari. Automated three-dimensional registration of medical images. *Medical Imaging V: Image Processing*, Proc. SPIE 1445:259–264, 1991.

[147] M. A. Oghabian and A. Todd-Pokropek. Registration of brain images by a multi-resolution sequential method. In A. C. F. Colchester and D. J. Hawkes, editors, *Information Processing in Medical Imaging 1991*, pages 165–174. Springer-Verlag, Berlin, 1991.

[148] A. Olivier, G. Bertrand, and C. Picard. Discovery of the first human stereotactic instrument. *Appl. Neurophysiol.*, 46:84–91, 1983.

[149] W. W. Orrison, L. E. Davis, G. W. Sullivan, F. A. Mettler, Jr., and E. R. Flynn. Anatomic localization of cerebral cortical function by magnetoencephalography combined with MR and CT. *AJNR*, 11:713–716, 1990.

[150] H. L. Oswal and S. Balasubramanian. An exact solution of absolute orientation. *Photogramm. Eng.*, 34:1079–1083, 1968.

[151] C. Pantev, M. Hoke, K. Lehnertz, B. Lütkenhöner, G. Fahrendorf, and U. Stöber. Identification of sources of brain neuronal activity with high spatiotemporal resolution through combination of neuromagnetic source localization (NMSL) and magnetic resonance imaging (MRI). *Electroencephalogr. Clin. Neurophysiol.*, 75:173–184, 1990.

[152] E. Peli, R. A. Augliere, and G. T. Timberlake. Feature-based registration of retinal images. *IEEE Trans. Med. Imaging*, 6:272–278, 1987.

[153] C. A. Pelizzari, G. T. Y. Chen, D. R. Spelbring, R. R. Weichselbaum, and C.-T. Chen. Accurate three-dimensional registration of CT, PET, and/or MR images of the brain. *J. Comput. Assist. Tomogr.*, 13:20–26, 1989.

[154] C. A. Pelizzari, K. K. Tan, D. N. Levin, G. T. Y. Chen, and J. Balter. Interactive 3D patient-image registration. In A. C. F. Colchester and D. J. Hawkes, editors, *Information Processing in Medical Imaging 1991*, pages 132–141. Springer-Verlag, Berlin, 1991.

[155] T. M. Peters, J. A. Clark, A. Olivier, E. P. Marchand, G. Mawko, M. Dieumegarde, L. Muresan, and R. Ethier. Integrated stereotaxic imaging with CT, MR imaging, and digital subtraction angiography. *Radiology*, 161:821–826, 1986.

[156] U. Pietrzyk, K. Herholz, and W.-D. Heiss. Three-dimensional alignment of functional and morphological tomograms. *J. Comput. Assist. Tomogr.*, 14:51–59, 1990.

[157] M. J. D. Powell. An efficient method for finding the minimum of a function of several variables without calculating derivatives. *Comput. J.*, 7:155–163, 1964.

[158] G. Prevost, J. Knoplioch, N. Treil, and C. Derosier. Procedure for validation of a planning method in neurosurgery. *Proc. Annu. Int. Conf. IEEE Eng. Med. Biol. Soc.*, 13:1123–1124, 1991.

[159] G. Rizzo, P. Pasquali, M. C. Gilardi, S. Cerutti, V. Bettinardi, G. Lucignani, G. Scotti, and F. Fazio. Multimodality biomedical image integration: Use of a cross-correlation technique. *Proc. Annu. Int. Conf. IEEE Eng. Med. Biol. Soc.*, 13:219–220, 1991.

[160] R. A. Robb. A software system for interactive and quantitative analysis of biomedical images. In K. H. Höhne, H. Fuchs, and S. M. Pizer, editors, *3D Imaging in Medicine: Algorithms, Systems, Applications*, pages 333–362. Springer-Verlag, Berlin, 1990.

[161] R. A. Robb, editor. *Visualization in Biomedical Computing 1992 (Proc. SPIE 1808)*. The Society of Photo-Optical Instrumentation Engineers, Bellingham, WA, 1992.

[162] R. A. Robb and C. Barillot. Interactive display and analysis of 3-D medical images. *IEEE Trans. Med. Imaging*, 8:217–226, 1989.

[163] D. W. Roberts, J. W. Strohbehn, J. F. Hatch, W. Murray, and H. Kettenberger. A frameless stereotaxic integration of computerized tomographic imaging and the operating microscope. *J. Neurosurg.*, 65:545–549, 1986.

[164] J. Rousseau, D. Gibon, P. Clarysse, J. P. Pruvo, S. Blond, and X. Marchandise. Une méthode de repérage stéréotaxique par IRM. *J. Med. Nucl. Biophys.*, 16:374–379, 1992.

[165] L. R. Schad, R. Boesecke, W. Schlegel, G. H. Hartmann, V. Sturm, L. G. Strauss, and W. J. Lorenz. Three dimensional image correlation of CT, MR, and PET studies in radiotherapy treatment planning of brain tumors. *J. Comput. Assist. Tomogr.*, 11:948–954, 1987.

[166] P. H. Schönemann. A generalized solution of the orthogonal Procrustes problem. *Psychometrika*, 31:1–10, 1966.

[167] P. H. Schönemann and R. M. Carroll. Fitting one matrix to another under choice of a central dilation and a rigid motion. *Psychometrika*, 35:245–255, 1970.

[168] G. H. Schut. On exact linear equations for the computation of the rotational elements of absolute orientation. *Photogrammetria*, 16:34–37, 1960.

[169] R. Sibson. Studies in the robustness of multidimensional scaling: Procrustes statistics. *J. R. Statist. Soc. B*, 40:234–238, 1978.

[170] R. L. Siddon. Prism representation: A 3D ray-tracing algorithm for radiotherapy applications. *Phys. Med. Biol.*, 30:817–824, 1985.

[171] M. Singh, W. Frei, T. Shibata, G. H. Huth, and N. E. Telfer. A digital technique for accurate change detection in nuclear medicine images: With application to myocardial perfusion studies using thallium-201. *IEEE Trans. Nucl. Sci.*, 26:565–575, 1979.

[172] E. A. Spiegel and H. T. Wycis. *Stereoencephalotomy*. Grune & Stratton, New York, 1952.

[173] E. A. Spiegel, H. T. Wycis, M. Marks, and A. J. Lee. Stereotaxic apparatus for operations on the human brain. *Science*, 106:349–350, 1947.

[174] D. Steiner and M. E. Kirby. Geometrical referencing of LANDSAT images by affine transformation and overlaying of map data. *Photogrammetria*, 33:54–75, 1977.

[175] H. Steinmetz, G. Furst, and H. Freund. Cerebral cortical localization: Application and validation of the proportional grid system in MR imaging. *J. Comput. Assist. Tomogr.*, 13:10–19, 1989.

[176] T. S. Sumanaweera, G. H. Glover, T. O. Binford, and J. R. Adler. MR susceptibility distortion quantification and correction for stereotaxy. *Biomedical Image Processing and Three-Dimensional Microscopy 1992*, Proc. SPIE 1660:30–43, 1992.

[177] K. R. Symon. *Mechanics*. Addison-Wesley Publishing Company, Reading, MA, 3rd edition, 1971.

[178] T. Takizawa. A neurosurgical navigation system employing MR images. *Toshiba Med. Rev.*, 34:10–18, 1990.

[179] J. Talairach and P. Tournoux. *Co-Planar Stereotactic Atlas of the Human Brain*. George Thieme Verlag, Stuttgart, 1988.

[180] J. D. Talbot, S. Marrett, A. C. Evans, E. Meyer, M. C. Bushnell, and G. H. Duncan. Multiple representations of pain in human cerebral cortex. *Science*, 251:1355–1358, 1991.

[181] J.-P. Thirion, A. Gourdon, O. Monga, A. Gueziec, and N. Ayache. Fully automatic registration of 3D CAT-scan images using crest lines. *Proc. Annu. Int. Conf. IEEE Eng. Med. Biol. Soc.*, 14:1888–1890, 1992.

[182] E. H. Thompson. An exact linear solution of the problem of absolute orientation. *Photogrammetria*, 15:163–179, 1958.

[183] K. D. Toennies, J. K. Udupa, G. T. Herman, I. L. Wornom, III, and S. R. Buchman. Registration of 3D objects and surfaces. *IEEE Comput. Graphics Appl.*, 10:52–62, 1990.

[184] J. K. Udupa and G. T. Herman, editors. *3D Imaging in Medicine*. CRC Press, Boca Raton, FL, 1990.

[185] P. A. Van den Elsen, J. B. A. Maintz, E.-J. D. Pol, and M. A. Viergever. Image fusion using geometrical features. *Visualization in Biomedical Computing 1992*, Proc. SPIE 1808:172–186, 1992.

[186] P. A. Van den Elsen, J. B. A. Maintz, and M. A. Viergever. Geometry driven multimodality image matching. *Brain Topogr.*, 5:153–158, 1992.

[187] P. A. Van den Elsen, E.-J. D. Pol, and M. A. Viergever. Medical image matching: A review with classification. *IEEE Eng. Med. Biol.*, 12:26–39, 1993.

[188] P. A. Van den Elsen and M. A. Viergever. Fusion of electromagnetic source data and tomographic image data. In H. U. Lemke, M. L. Rhodes, C. C. Jaffe, and R. Felix, editors, *Computer Assisted Radiology 1991*, pages 240–246. Springer-Verlag, Berlin, 1991.

[189] P. A. Van den Elsen and M. A. Viergever. Marker guided registration of electromagnetic dipole data with tomographic images. In A. C. F. Colchester and D. J. Hawkes, editors, *Information Processing in Medical Imaging 1991*, pages 142–153. Springer-Verlag, Berlin, 1991.

[190] P. A. Van den Elsen, M. A. Viergever, A. C. Van Huffelen, W. Van der Meij, and G. H. Wieneke. Accurate matching of electromagnetic dipole data with CT and MR images. *Brain Topogr.*, 3:425–432, 1991.

[191] P. Van Wie and M. Stein. A LANDSAT digital image rectification system. *IEEE Trans. Geosci. Electronics*, 15:130–137, 1977.

[192] A. Venot, J. Y. Devaux, M. Herbin, J. F. Lebruchec, L. Dubertret, Y. Raulo, and J. C. Roucayrol. An automated system for the registration and comparison of photographic images in medicine. *IEEE Trans. Med. Imaging*, 7:298–303, 1988.

[193] A. Venot, J. F. Lebruchec, and J. C. Roucayrol. A new class of similarity measures for robust image registration. *Comput. Vision Graphics Image Processing*, 28:176–184, 1984.

[194] A. Venot and V. Leclerc. Automated correction of patient motion and gray values prior to subtraction in digitized angiography. *IEEE Trans. Med. Imaging*, 3:179–186, 1984.

[195] A. Venot, J. C. Liehn, J. F. Lebruchec, and J. C. Roucayrol. Automated comparison of scintigraphic images. *J. Nucl. Med.*, 27:1337–1342, 1986.

[196] G. Wolberg. *Digital Image Warping.* IEEE Computer Society Press, Los Alamitos, CA, 1990.

[197] R. Y. Wong. Sensor transformations. *IEEE Trans. Syst. Man Cybern.*, 7:836–841, 1977.

[198] T. Yamamoto, S. J. Williamson, L. Kaufman, C. Nicholson, and R. Llinas. Magnetic localization of neuronal activity in the human brain. *Proc. Natl. Acad. Sci. USA*, 85:8732–8736, 1988.

[199] M. Yanagisawa, S. Shigemitsu, and T. Akatsuka. Registration of locally distorted images by multiwindow pattern matching and displacement interpolation: The proposal of an algorithm and its application to digital subtraction angiography. In *Proc. 7th Int. Conf. Pattern Recognition*, pages 1288–1291, 1984.

[200] J. J.-H. Yu, B.-N. Hung, and C.-L. Lious. Fast algorithm for digital retinal image alignment. *Proc. Annu. Int. Conf. IEEE Eng. Med. Biol. Soc.*, 11:374–375, 1989.

[201] J. Zhang, M. F. Levesque, C. L. Wilson, R. M. Harper, J. Engel, Jr., R. Lufkin, and E. J. Behnke. Multimodality imaging of brain structures for stereotactic surgery. *Radiology*, 175:435–441, 1990.

[202] G. Zubal, H. Tagare, L. Zhang, and J. Duncan. 3-D registration of intermodality medical images. *Proc. Annu. Int. Conf. IEEE Eng. Med. Biol. Soc.*, 13:293–294, 1991.

Medical Image Registration: a Review. Francisco P. M. Oliveira, JoÃ£o Manuel R. S. Tavares. Faculdade de Engenharia da Universidade do Porto / Instituto de Engenharia MecÃ¢nica e GestÃ£o Industrial, Rua Dr. Roberto Frias, 4200-465 Porto, Portugal.Â Abstract This paper presents a review of automated image registration methodologies that have been used in the medical field. The aim of this paper is to be an introduction to the field, provide knowledge on the work that has been developed and to be a suitable reference for those who are looking for registration methods for a specific application. Ac-quiring and preparing data for image registration, correctingscanner errors, and detecting algorithm failure are also discussedin this section. Section II discusses rigid body registration appli-cations: serial MRI, functional MRI, registration of PET andMRI, registration of MRI and CT, registration of nuclear medi-cine, and registration in guided therapeutic procedures. SectionIII is devoted to nonrigid registration: concepts, algorithms, ap-plications, cohort studies, and biomechanical models for im-age-guided neurosurgery applications.The first section of the book appears to be targeted